RIGA TECHNICAL UNIVERSITY

Juris Bitenieks

CARBON NANOTUBE BASED THERMOPLASTIC POLYMER COMPOSITES

Summary of the Doctoral Thesis

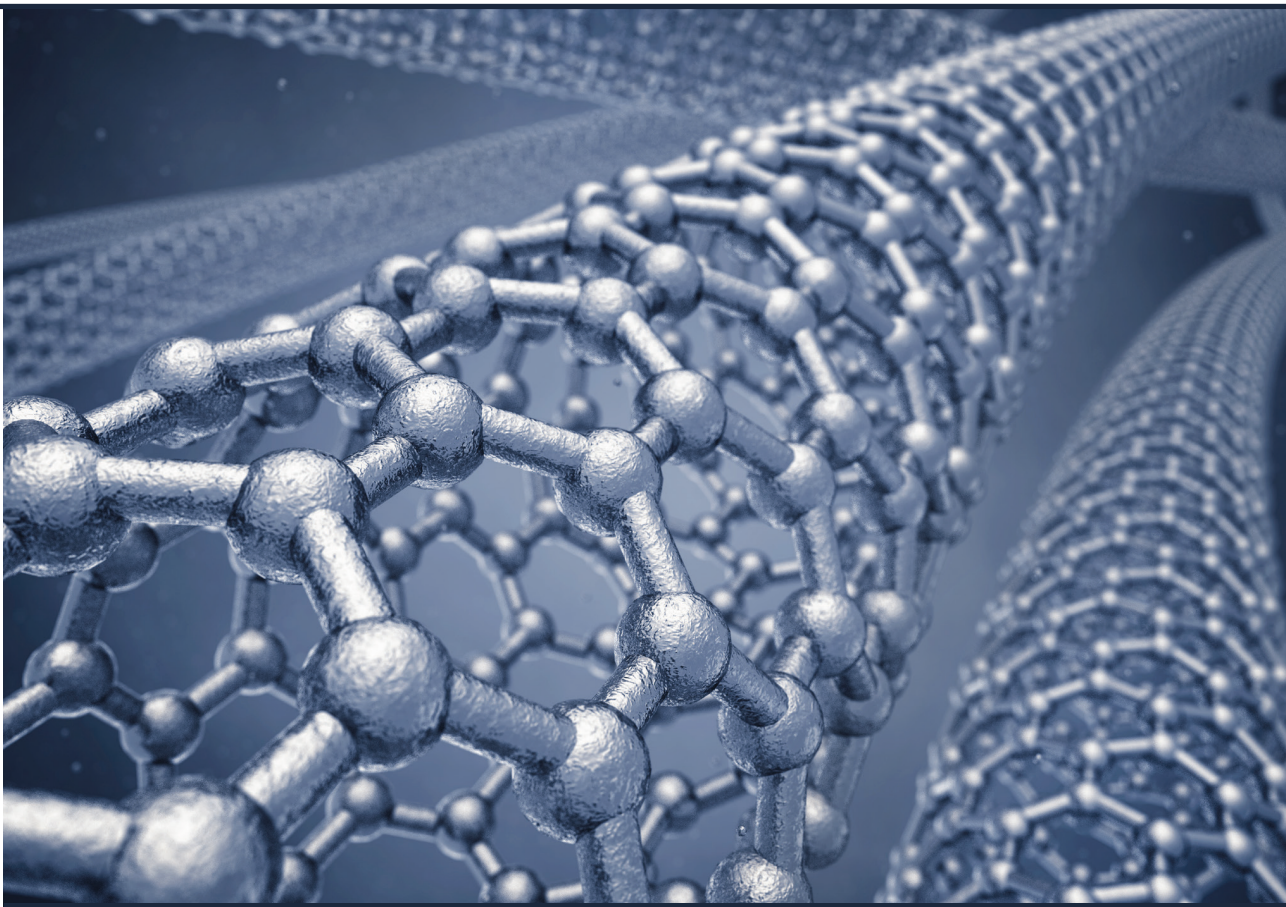

RTU Press
Riga 2018

RIGA TECHNICAL UNIVERSITY
Faculty of Materials Science and Applied Chemistry
Institute of Polymer Materials

Juris BITENIEKS
Doctoral Student of the Study Programme "Chemical Technology"

CARBON NANOTUBE BASED THERMOPLASTIC POLYMER COMPOSITES

Summary of the Doctoral Thesis

Scientific supervisors
Professor Dr. habil. sc. ing.
MĀRTIŅŠ KALNIŅŠ
Lead Researcher Dr. sc. ing.
JĀNIS ZICĀNS

RTU Press
Riga 2018

Bitenieks J. Carbon Nanotube Based Thermoplastic Polymer Composites. Summary of the Doctoral Thesis. Riga: RTU Press, 2018. 38 p.

Published in accordance with the decision of the Promotion Council „RTU P-02" of 20 December, 2017.

This work has been supported by the European Social Fund within the project «Support for the implementation of doctoral studies at Riga Technical University».

ISBN 978-9934-22-053-1
ISBN 978-9934-22-054-8 (pdf)

DOCTORAL THESIS PROPOSED TO RIGA TECHNICAL UNIVERSITY FOR THE PROMOTION TO THE SCIENTIFIC DEGREE OF DOCTOR OF ENGINEERING SCIENCES

To be granted the scientific degree of Doctor of Engineering Sciences, the present Doctoral Thesis has been submitted for the defence at the open meeting of RTU Promotion Council on March 7, 2018 at the Faculty of Materials Science and Applied Chemistry of Riga Technical University, 3 Paula Valdena Street, Room 272.

OFFICIAL REVIEWERS

Professor Dr. sc. ing. Jurijs Ozoliņš
Rīga Technical University

Professor Dr. habil. phys. Andris Šternbergs
University of Latvia

Lead Researcher Dr. chem. Bruno Andersons
Latvian State Institute of Wood Chemistry

DECLARATION OF ACADEMIC INTEGRITY

I hereby declare that the Doctoral Thesis submitted for the review to Riga Technical University for the promotion to the scientific degree of Doctor of Engineering Sciences is my own. I confirm that this Doctoral Thesis had not been submitted to any other university for the promotion to a scientific degree.

Juris Bitenieks …….
Date: ……

The Doctoral Thesis has been written in Latvian. It consists of Introduction; 3 chapters; Conclusion; 2 appendices; 124 figures; 29 tables; 30 equations. The total number of pages is 179. The Bibliography contains 357 titles.

ACKNOWLEDGMENT

I am deeply grateful to my scientific supervisors Professor Mārtiņš Kalniņs, Lead Researcher Jānis Zicāns and Professor Remo Merijs Meri for immense interest and motivation as well as for valuable advice and dedicated time during writing the Thesis. I also express my gratitude for the opportunity to use the laboratories of RTU Polymer Materials Institute and a wide range of research equipment for carrying this work out.

Many thanks to the friendly colleagues from the RTU Institute of Polymer Materials, who cheered me up and shared their knowledge during the development of the Doctoral Thesis.

Thanks to Professor Robert Maksimov from LU Institute of Polymer Mechanics for helping with characterization of mechanical properties.

Thanks to researcher Kārlis Kundziņš form LU Institute of Solid State Physics for microscopy investigation.

Sincere thanks to my family and friends for motivation and support.

CONTENTS

ABBREVIATIONS AND SYMBOLS

a	thermal diffusivity
AC	alternating current
A_T	impact strength
c	specific heat capacity
CNT	carbon nanotube
DC	direct current
DMTA	dynamic mechanical thermal analysis
DSC	differential scanning calorimetry
E	tensile elastic modulus
E'	storage modulus
E''	loss modulus
f	frequency
F	force
G'	melt storage modulus
H_V	Vikers hardness
MWCNT	multiwall carbon nanotube
n_{tec}	flow index
PE	polyethylene
PET	polyethylene terephthalate
PP	polypropylene
PVAc	polyvinyl acetate
SAC	styrene-acrylate copolymer
SEM	scanning electron microscopy
tanδ	loss tangent
T	temperature
T_g	glass transition temperature
TGA	termogravimetric analysis
T_m	melting temperature
US	ultrasound
ε	strain
ε_B	tensile strain at break
ε_Y	tensile strain at yield
η*	complex viscosity
λ	thermal conductivity
σ	tensile stress
σ'	AC conductivity
σ_B	tensile strength at break
σ_Y	tensile yield strength
ω	angular frequency

GENERAL OVERVIEW OF THE DOCTORAL THESIS

Introduction

Polymers as a materials are characterized by a wide range of practically useful properties. Among them are low density, relatively high strength, easy processability, etc.

Existing experience suggests that the spectrum of polymer qualities can be significantly expanded to form heterogeneous composite materials on their basis.

One of the most promising fillers in recent years in polymer matrix composites are carbon nanotubes (CNTs). The available information on CNT containing polymer compositions suggests that already a small content of CNTs not only significantly improves the stress-strain properties of polymers, but also gives them new unrivaled properties, such as increasing their electro and thermal conductivity. However, in order to maximally evaluate obtaining possibilities of CNT containig polymer composites and their properties, polymers by different nature were selected with different structure and stress-strain parameters:

1) polyvinyl acetate (PVAc) and styrene-acrylate copolymer (SAC) water dispersions, by using them it is possible to obtain polymer/CNT nanocomposites with low CNT content (up to 2 wt. %) and good CNT dispersion in the free space between polymer particles;

2) polyethylene (PE), polypropylene (PP) and polyethylene terephthalate (PET), widely used thermoplastic, semi-crystalline polymers, which together make up the bulk of the world's used range of polymers. The formation of nanocomposites containing CNT with these polymers opens up the possibilities to expand their specific applications in structural materials, packaging materials and electronics.

Aim of the Doctoral Thesis

The objective of the Doctoral Thesis is to obtain CNT containing polymer composites from various thermoplastic polymers (PVAc, SAC, PE, PP, PET) using different polymer states in the CNT and polymer mixing process: polymer water dispersion and polymer in a molten state.

To investigate the influence of polymer nature and composite production conditions on the most important structural characteristics and properties of composite.

Tasks of the Doctoral Thesis

1. Development of CNT/polymer nanocomposite production methodology from polymer water dispersion (PVAc and SAC polymer matrix) and polymer melt (PE, PP and PET polymer matrix).
2. Development and improvement of methodology for the production of the obtained systems for the study of composite structure, as well as for determination of stress-strain, rheological, dielectric and other properties.
3. Evaluation of the relationship between the characteristics of nanocomposite structure and the most important properties.

Scientific novelty of the Doctoral Thesis

Obtained carbon nanotube containing polymer composites with different nature thermoplastic polymer matrix structure characteristics parameters and connection of stress-strain, thermal, dielectric, rheological, etc. properties have been evaluated by various methods. Characteristics of these properties are determined by the composite morphology at nano and micro level.

The methods used to obtain composites can produce composites with specific morphological features. Carbon nanotubes in the polymer matrix form bundles and their spatial network sets that reinforce the polymer matrix while simultaneously changing the thermal, dielectric, and rheological properties of nanocomposites.

It is proven that by using the Mori-Tanaka mathematical model it is possible to describe dependence of nanocomposite elastic modulus on the content and orientation of nanoparticles.

Practical importance of the Doctoral Thesis

Methods were developed for obtaining CNT containing composites for a wide range of thermoplastic polymer matrices by using different polymer states in the CNT polymer combining process: polymer water dispersion and polymer melt.

It was proved that it is possible to achieve a satisfactory level of CNT dispersion in a composite with all studied polymers and their working conditions by basically using traditional polymer processing techniques.

It has been shown that by introducing small ammounts of CNT (up to 2 wt. %) in thermoplastic polymer matrices, it is possiblr to obtain composites with increased stress-strain properties (tensile elastic modulus and yield strength enhancement increases by 1.6 and 1.7 times, flexural elastic modulus increases 1.3 times and hardness increases 1.4 times). Electrical conductivity increases significantly 10^2–10^5 times, as a result nanocomposites become conductive materials. Thermal conductivity, depending on the polymer matrix, increases 1.2–1.7 times.

Thesis statements to be defended

1. By purposefully creating polymer systems with a small CNT filler content (0.01–5 wt. %) from PVAc and SAC water dispersions, as well as temoplast polymers PE, PP and PET, it is possible to obtain nanocomposites with a wide range of stress-strain, thermal, dielectric and rheological set of properties.
2. In the process of obtaining polymer/CNT systems, CNTs in the polymer matrix create structures of interconnected bundle network, which performs reinforcement, electric conductivity and heat conduction functions.
3. The obtained polymer/CNT systems that consist of two different materials – polymer matrixes and CNT filler, show a percolation treshold at certain CNT concentrations, which characterizes the concentration of filler at which it significantly alters dielectric and rheological properties.

4. CNTs change the crystalline structure of the semi-crystalline polymers (PE, PP, PET), creating additional nucleation sites. As a result, crystals with a large size distribution are formed during the crystallization process.

Approbation of the Doctoral Thesis

The main results of the Doctoral Thesis were presented at twenty one international conference, seven full text scientific publications and seven reviewed full text scientific conference theses have been published.

SUMMARY OF LITERATURE REVIEW

In 1991, S. Iijima [1] discovered multiwall carbon nanotubes (MWCNTs) in carbon soot by applying arc discharge to the graphite. MWCNT consists of two or more concentric cylindric graphite sheet hulls that are coaxially located around empty central hull. Between adjanced MWCNT walls are acting Van der Waals forces. The spacing between the walls is 0.34–0.36 nm which is close to the distance between carbon atoms in graphite lattice. Average diameter of CNT is a few dozen of nanometers [2]. The CNT structure with strong σ bonds between carbon atoms gives them very high tensile elastic (E) modulus and tensile strength. In turn, the high strength of bonds in plane along CNT cylindrical axis provides it with excellent resistance to tensile break.

By taking into account the potential properties of CNTs, a very extensive studies have been carried out on the CNT/polymer nanocomposite manufacturing direction for functional and structural applications. However, the full potential of the CNTs as a polymer matrix reinforcement is very limited due to the difficulties of CNT agglomerate dispersion during the composite processing. The problems of CNT dispersion are different from other conventional fillers such as spherical particles and fibers (carbon black, clay, fiberglass, etc.), since CNTs has specific properties such as small diameters on a nanosized scale with a large length/diameter (l/d) ratio (> 1000) and high surface energy [3].

Deposition from an emulsion, suspension or solution is one of the most commonly used methods to obtain CNT/polymer nanocomposites because it is suitable for preparation of small amounts of samples. This method is commonly used to make composite films [4]. Melt processing is preferred for industrial CNT/polymer nanocomposites manufacturing because of its low cost, and it is possible to easy deliver large-scale commercial production. Melt mixing is simple and compatible with traditional polymer processing methods, such as extrusion, injection molding, roll milling and compression molding.

At present the main challenge in obtaining polymer nanocomposites is the successful transfer of CNT characteristic mechanical and conductivity properties to macroscopic scale composite materials. The biggest problem in achieving this is the CNT dispersion. Effective load transfer cannot be achieved if the CNT agglomerates remain in the polymer matrix; it is necessary to spatially disperse CNT in bundles or in an isolated condition. The CNT reinforcement effect in the composites is determined by the CNT dispersion, l/d ratio, the spatial

position of the filler and the interphase effect between the CNTs and the polymer matrix [5]. By overcoming these difficulties, it is possible to obtain polymer composite materials with improved mechanical properties and to increase their electrical and thermal conductivity.

MATERIALS AND METHODS

For polymer/CNT nanocomposite matrix materials were used commercially consumer grade semi-crystalline polymers (PE, PP, PET) and polymer water dispersions (PVAc, SAC). The used polymers and their tensile properties – elastic modulus (E), tensile strength (σ_B), tensile deformation (ε_B), yield strength (σ_Y) and yield deformation (ε_Y), are shown in Table 1.

Table 1

Polymer matrices

Thermoplastic polymers		
Designation	Chemical structure	Tensile parameters
Medium density polyethylene (PE) *Egyeuroptene MD 3804 U*		E = 610 MPa σ_B = 11 MPa ε_B = 670 % σ_Y = 16 MPa ε_Y = 13 %
Polypropylene (PP) *56M10*	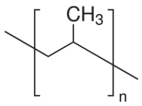	E = 937 MPa σ_B = 15 MPa ε_B = 570 % σ_Y = 21 MPa ε_Y = 5 %
Polyethylene terephthalate (PET) *Lighter C93*	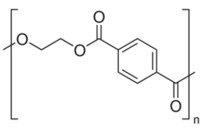	E = 2182 MPa σ_B = 34 MPa ε_B = 310 % σ_Y = 64 MPa ε_Y = 4 %
Polymer water dispersions		
Polyvinyl acetate (PVAc) *FINNDISP HW 1*	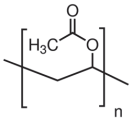	E = 1610 MPa σ_B = 15 MPa ε_B = 540 % σ_Y = 8 MPa ε_Y = 3 %
Styrene-acrylate copolymer (SAC) *FINNDISP A 10*	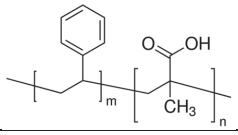	E = 1690 MPa σ_B = 14 MPa ε_B = 670 % σ_Y = 7 MPa ε_Y = 5 %

MWCNTs and various types of commercial MWCNT/polymer masterbatches were used as polymer matrix modifying fillers. The typical characteristics of the MWCNT filler materials and modified polymer matrices are presented in Table 2.

Table 2

MWCNT fillers

Designation	Main parameters	Structure	Matrix
Baytubes C 150 P MWCNT agglomerates Sample designation: PVAc/CNT SAC/CNT PE/CNT	Outer diameter: 13–16 nm Inner diameter: 4 nm Length: 1–10 μm	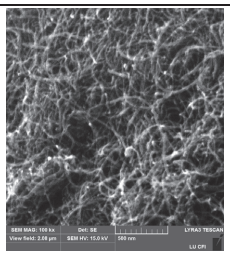	PVAc SAC PE
Nanocyl 9000 polyethylene predispersed *Nanocyl 7000* MWCNT concentrate Sample designation: PE/Nanocyl	MWCNT content: 31.6 % Outer diameter: 9.5 nm Length: 1.5 μm T_m = 130 ºC	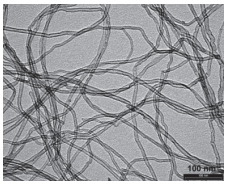	PE
MB3020–01 polypropylene predispersed MWCNT concentrate Sample designation: PP/CNT	MWCNT content: 20.39 % Outer diameter: 10 nm Length: >10 μm T_m = 162 ºC	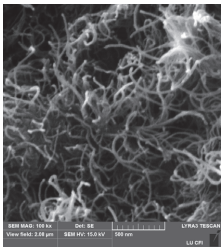	PP
MB6815–00 polyethylene terephthalate predispersed MWCNT concentrate Sample designation: PET/CNT	MWCNT content: 15 % Outer diameter: 10 nm Length: >10 μm T_m = 250 ºC	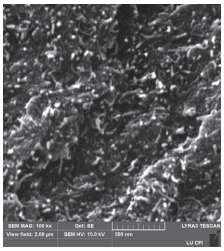	PET

Depending on the type of the used polymer matrix for CNT containing polymer nanocomposites, the melt processing and solution casting methods were used.

1) PE, PP and PET nanocomposites were obtained by mixing CNTs in polymer melt by using two roll mills and extrusion. Test samples were made by injection molding and compression molding.

2) PVAc and SAC matrix nanocomposites were obtained by dispersing CNTs in water by ultrasound (US) and then mixing with polymer dispersions. To stabilize CNT water dispersion a surfactant – sodium dodecyl sulphate was used. The CNT dispersion in water was stabilized with surfactant. Test samples were made by casting nanocomposite films.

The nanocomposite processing scheme is shown in Fig. 1.

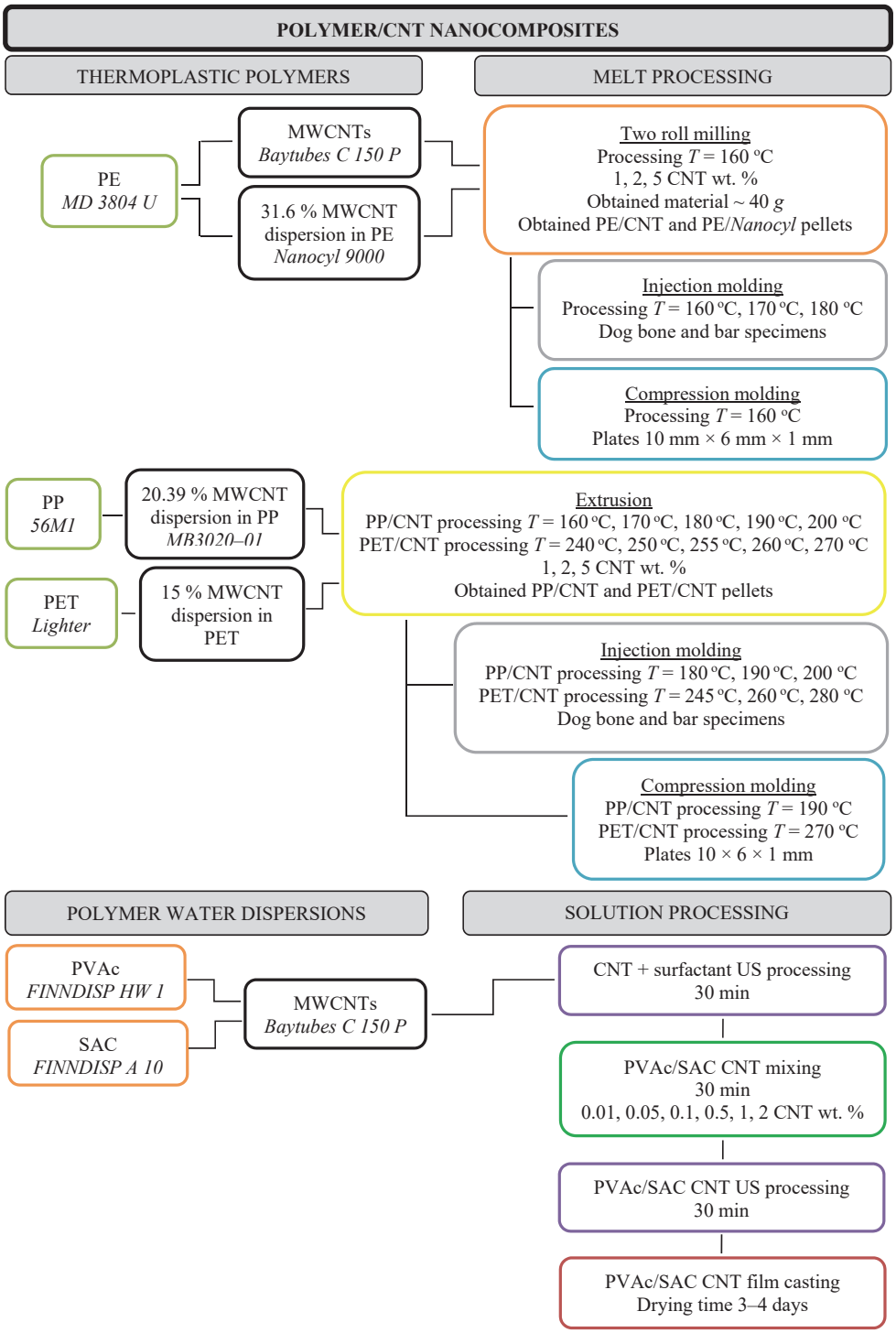

Fig. 1. Polymer nanocomposite processing scheme.

The used research methods, equipment and the determined parameters for the obtained polymer/CNT nanocomposites are shown in Table 3.

Table 3

Evaluation methods of polymer/CNT nanocomposites

Evaluation method	Equipment	Determined parameters
Morphology	Scanning electron microscope *Tescan Lyra3 XM*	Surface structure of sample cryofracture
Density	Hydrostatic weighing equipment *YDK 01* in combination with *Sartorius KB BA 100* electronic balance	Density ρ
Stress-stain properties	*Zwick/Roell* materials testing device *BDO–FB020TN*	Stress-stain parameters in tensile: tensile elastic modulus E, tensile yield strength σ_Y, tensile strain at yield ε_Y, tensile strength at break σ_B, tensile strain at break ε_B and in flexure: flexural elastic modulus E_f and maximum stress σ_{fmax}
Vickers microhardness	Microhardness microscope *Vickers M–41*	Microhardness H_V
Charpy impact strength	*Zwick 24*	Impact strength A_T, impact energy E and impact force F
Creep properties	Flexural and tensile creep stand	Long-term and short-term creep deformation $\varepsilon_{\%}$
Dynamic mechanical thermal analysis	*Mettler Toledo DMA/SDTA861*	Dynamic mechanical properties in tensile: storage modulus E', loss modulus E'' and loss tangent tanδ
Differential scanning calorimetry	*Mettler Toledo DSC 1/200W*	Glass transition temperature T_g, initial melting temperature $T_{s\,m}$, maximum melting temperature T_m, final melting temperature $T_{b\,m}$ and melting enthalpy ΔH for determination of crystallinity degree
Thermogravimetric analysis	*Mettler Toledo TGA1/SF*	Changes of sample mass %
Thermal properties	*NETZSCH LFA 447 NanoFlash*	Thermal diffusivity a, specific heat capacity c and thermal conductivity λ
Dielectric Properties	Broadband dielectric spectrometer *Novocontrol Concept 50*	Relative permittivity ε', dielectric loss ε'' and AC conductivity σ'
Melt rheology	Rotational rheometer *REOLOGICA StressTech NOVA*	Complex viscosity of melt η*, storagea G' and loss G'' modulus

EVALUATION OF MAIN RESULTS

1. Morphology studies

Structure of polymer matrices obtained by the solution method

By using the PVAc dispersion as a matrix, the resulting film structure is formed from coalescent microscopic polymer particles (Fig. 2). Particle coalescence [6] has occurred during the film formation by evaporation of the solvent and polymer particles getting closer to each other, eventually forming a tightly ordered structure. From SAC polymer dispersion obtained films, coalescence was not observed because SAC particles are 30–40 times smaller in size than PVAc particles and SAC polymer dispersion is stabilized with anionic sufactant. As a result, when the film is formed, SAC particles more evenly grow together without leaving a significant interlayer.

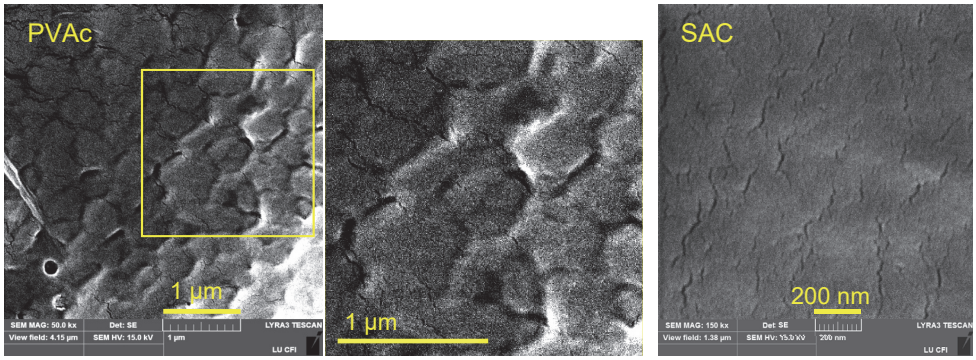

Fig. 2. SEM microphotographs of PVAc and SAC polymer matrices.

Structure of polymer/CNT nanocomposites

During PVAc/CNT nanocomposite film formation (Fig. 3), CNTs always occupy the space between PVAc particles. However, simultaneously existing CNT agglomerates break down the PVAc particle arrangement and PVAc coalescence disappears. When looking at the other polymer/CNT nanocomposites, it is possible to observe a uniform CNT dispersion in a polymer matrix at the breakage site of the sample, which is indicated by the partially pulled out endings of CNT bundles. Among homogeneously dispersed individual CNTs, it is possible to distinguish between existing CNT agglomerates and the elements of twisted CNT bundle reinforcement structure.

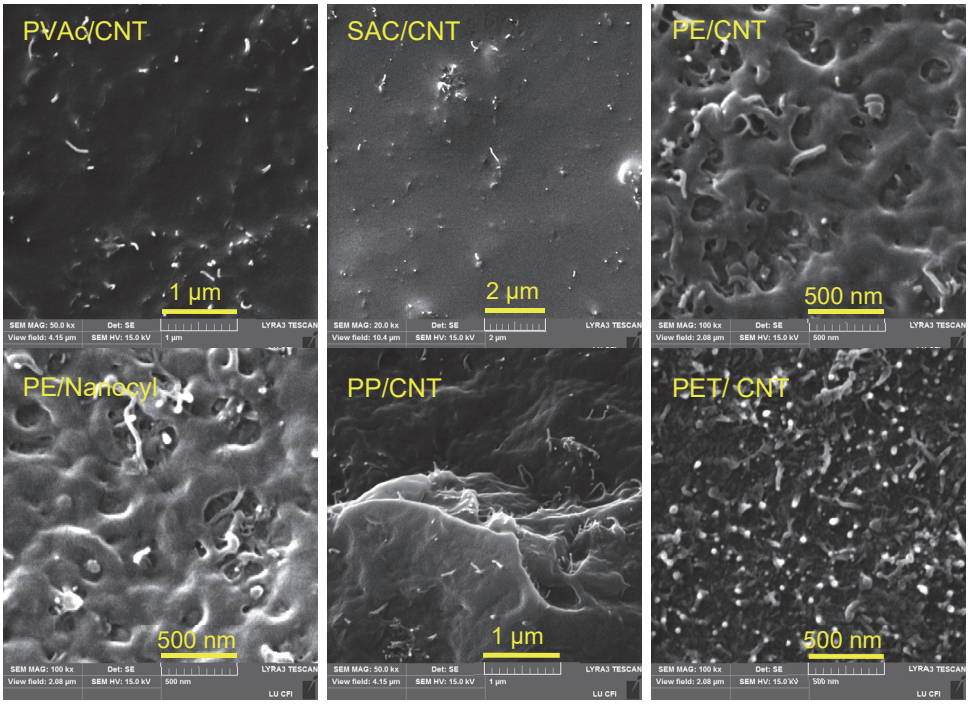

Fig. 3. SEM microphotographs of polymer/CNT nanocomposites.

The CNT reinforcement formation scheme is shown in Fig. 4. During the dispersion and mixing process of CNTs, the CNT agglomens are split into a lot smaller, twisted CNT bundles. When the CNTs are mixed in the polymer matrix, the CNT bundles are stretched under the influence of shear forces and the CNTs are oriented towards the flow direction. These bundles, twisted by individual CNTs, form units of connected CNT bundles that provide polymer matrix reinforcement. Depending on the size of the bundles (Fig. 4 c), the largest bundles are not able to completely fill with polymer macromolecules, as a result leaving air vacancies in obtained composite materials that affects their physical properties.

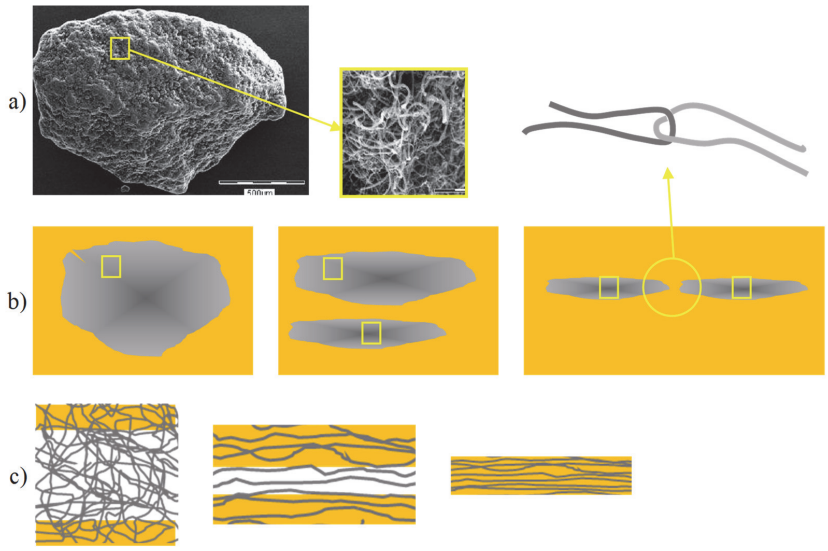

Fig. 4. CNT agglomerate (a), CNT bundles developed from CNT agglomerate (b), that reinforce polymer matrix (c).

2. Mechanical properties

Tensile properties of polymer matrices

The structure of PVAc, SAC, PE, PP and PET matrices is substantially different, respectively the stress-strain parameters of these matrices also differ significantly, as can be seen from the stress-strain curves in Fig. 5. Thereby CNT reinforcement mechanism and the reinforcement result for the obtained polymer/CNT nanocomposites is different. In the case of PVAc and SAC polymers, the load is beared by coalescing polymer particles, which take up a total composite volume. The bearing capacity of this volume is determined by the relationship between particles, where the major role plays the interparticle diffusive boundary layers where CNT bundles insert. In the case of PE, PP and PET, the mechanical load is beared by the polymer matrix crystalline frame the volume of which doesn't exceed 36 %, 33 % and 24 % and CNTs occupies a space in the amorphous phase.

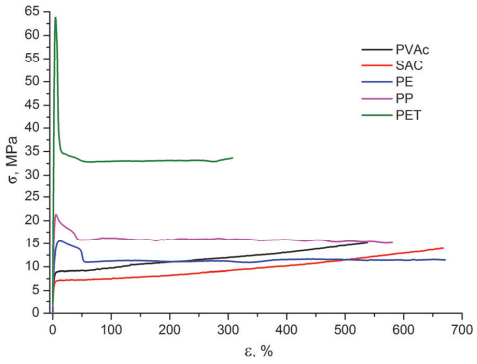

Fig. 5. Polymer matrix tensile σ(ε) curves.

Tensile properties of nanocomposites obtained by solution processing

PVAc/CNT and SAC/CNT nanocomposite stress-strain parameters (Fig. 6) show a gradual decrease in relative deformation as the CNT concentration in the matrix increases. At the same time, the addition of CNTs to PVAc and SAC matrices significantly improves their strength

parameters. It is indicated by the increase in PVAc/CNT and SAC/CNT nanocomposite tensile parameters (E, σ_Y and σ_B).

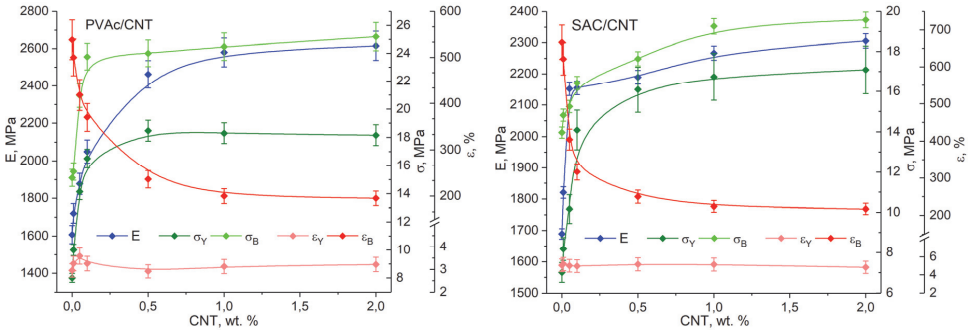

Fig. 6. PVAc/CNT and SAC/CNT nanocomposite tensile parameter E, σ_Y, σ_B, ε_Y and ε_B dependence on CNT concentration.

By adding a small amount (up to 0.5 wt. %) of CNTs, very steep increase in E, σ_Y and σ_B is observed; for PVAc/CNT nanocomposites E increases by 53 %, σ_Y and σ_B increases by 131 % and 47 %, but for SAC/CNT nanocomposites these parameters at 0.5 wt. % CNT concentration increased by 30 %, 130 % and 26 %. This points to the reinforcing effect of CNTs and the simultaneous effect on PVAc and SAC macromolecules, limiting their mobility. At higher CNT concentrations, E and σ_B increase sharply reduces, but σ_Y values for PVAc/CNT nanocomposites even slightly decrease.

Modelling of PVAc/CNT nanocomposite elastic properties

In order to theoretically model the mechanical properties of the obtained nanocomposites, the theory of elasticity was used [7]. A tensor of elasticity (C^*) was determined according to the Eshelby's equation (1) for a composite of low-concentration, uniaxially oriented or one-dimensional (1D) ellipsoidal inclusions [8]:

$$C^* = C^m + V_f \left(C^f - C^m\right) \cdot\cdot A^f \tag{1}$$

$$A^f = A_{dilute} = \left[I + S \cdot\cdot \left(C^f - C^m\right) \cdot\cdot \left(C^m\right)^{-1}\right]^{-1} \tag{2}$$

where V_f CNT volume fraction;
A^f strain concentration tensor;
C^f rigidity tensor of CNT filler;
C^m rigidity tensor of matrix material;
S Eshelby's tensor;
I fourth-rank unit tensor with the components:

$$I_{ijkl} = \frac{1}{2}\left(\delta_{ik}\delta_{jl} + \delta_{il}\delta_{jk}\right) \tag{3}$$

where δ_k is Kronecker symbol.

However, at high nanoparticle concentration it can no longer be assumed that the filler particles are uniformly dispersed in the polymer matrix. Therefore, it is not possible to use theoretical calculation models, where under conditions the composite should have a homogeneous structure and filler particles with a specific *l*/*d* ratio. In the case of finite nanoparticle concentrations and taking into account their elastic interaction with a composite, the Mori-Tanaka model (4) can be applied according to which tensor A^f is expressed in the following form [9]:

$$A^f = A_{MT} = A_{dilute} \cdot \left[(1 - V_f) I + V_f A_{dilute} \right]^{-1} \quad (4)$$

where A_{MT} and A_{dilute} are strain concentration tensors according to Mori-Tanaka and Eshelby.

The tensor of effective rigidity C_{ijkl} (5) of a composite with a random CNT orientation was obtained by averaging the rigidity tensor C^* of the structural element over all spatial directions in the composite [10]:

$$C_{ijkl} = \frac{1}{30}\left[2(2C^*_{mmnn} - C^*_{mnmn})\delta_{ij}\delta_{kl} + (3C^*_{mnmn} - C^*_{mmnn})(\delta_{ik}\delta_{jl} + \delta_{il}\delta_{jk})\right]. \quad (5)$$

By using the component C^*_{ijkl} calculation formulas, the expressions for elastic constants were obtained, respectively, the elastic modulus *E*, the shear modulus *G*, and the Poisson's ratio ν. To evaluate the effect of the CNT orientation on the elastic properties of the composition, one-dimensional orientation (1D) of CNTs and chaotic orientation in the plane (2D) and in space (3D) were modeled. Figure 7 shows PVAc/CNT nanocomposite *E* values at CNT content of 0.1 (a), 1 (b) and 2 (c) wt. % at different CNT orientation in composite.

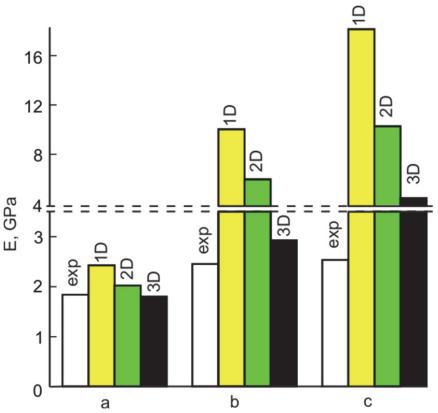

Fig. 7. Experimental (exp) and theoretical *E* values of PVAc/CNT nanocomposite at different CNT orientation in composite at 0.1 (a), 1 (b) and 2 (c) CNT wt. %.

The calculated values of *E* are located closest to the experimental values at CNT content of 0.1 wt. % in the case of 3D orientation. At higher CNT content, the difference between experimental and calculated *E* values increases. For example, at CNT concentration of 2 wt. %, calculated *E* values for 1D, 2D, and 3D CNT orientation exceeded the experimental data by 7.4, 4.1 and 2.4 times, respectively. Hence the initial assumptions of the rectilinear form and completely uniform dispersion of CNTs in the matrix do not allow to describe the experimental *E* dependence on CNT concentration. Therefore, the CNT agglomeration variant was considered – it was assumed that part of the CNTs are uniformly dispersed in the matrix, while the remaining CNTs are agglomerated:

$$V_f = V_{fd} + V_{fa} \quad (6)$$

where V_f is CNT volume content, V_{fd} and V_{fa} are dispersed and agglomerated CNT volume content.

To describe the agglomerated and dispersed CNTs, a coefficient $k = V_{fa}/V_f$ was introduced which describes agglomerated CNT relative part in the composite: at $k = 0$, all CNTs are uniformly dispersed in the polymer matrix and at $k = 1$, all CNTs are agglomerated. In the calculations it was assumed that the agglomerates are spherical. Similarly, as [11], where the clusters of curved CNTs are modelled by separate linear segments with a l/d ratio much smaller than for straight CNTs. At these calculations the curved CNT shape in the agglomerate was replaced by zigzag shape having a random spatial orientation.

The effective elastic constants of the agglomerate depend on the CNT volume fraction μ_{fa} and CNT linear segment l/d ratio in the agglomerate. The volume content of agglomerates V_a in a composite can be determined by the formula

$$V_a = \frac{V_{fa}}{\mu_{fa}} = \frac{kV_f}{\mu_{fa}}. \tag{7}$$

The variation in the coefficient k of partial agglomeration of CNTs can be found from the relationship between the experimental and calculated E values of the composite. The effective elastic constants of the agglomerate were calculated at $\mu_{fa} = 0.5$ and CNT linear segment size ratio equal to 20. Then, for certain V_f values, values of k were taken in the range $0 \le k \le 1$ and by using the equation (7) V_f values were found and elastic constants of the composite containing only agglomerates were calculated, neglecting the quantity V_{fd}. Further, the composite was assumed as a matrix material filled with dispersed CNTs, its E modulus was calculated and the obtained results were compared with the experimental results. In the case of discrepancies between these data, the calculations were repeated at other k values until an acceptable coincidence between the calculations and the experiments was achieved.

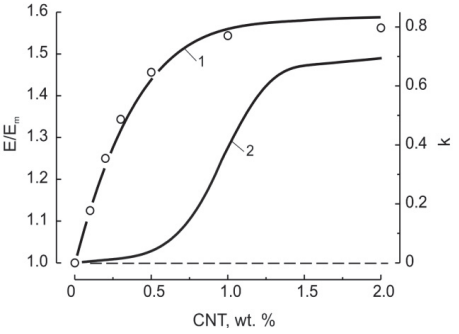

Fig. 8. PVAc/CNT nanocomposite relative elastic modulus E/E_m depending on CNT concentration.

The results of the analysis are shown in Fig. 8, where the points fit to the experimental values for the relationship between the E values of the composite and the matrix E_m. The calculated E/E_m ratio, depending on the CNT content (curve 1), was obtained at the nonmonotonic variation of the coefficient k of the CNTs (curve 2). It is obvious that at over 0.5 wt. % CNT content, CNT agglomerate fraction begins to grow rapidly and at 2 wt. % reaches ~70 % of their total content in the composite.

Tensile properties of nanocomposites obtained by melt processing

The PE/CNT and PE/*Nanocyl* nanocomposites demonstrate semi-crystalline polymer $\sigma(\varepsilon)$ relationship with pronounced overlap peak (σ_Y) formation in the transition region from elastic to plastic deformation. At 5 wt. % CNT, samples break right after this overlap area with no plastic deformation at constant stress. On the other hand, by the affect of CNTs nanocomposite E, σ_Y and σ_B parameters gradually increase (Fig. 9).

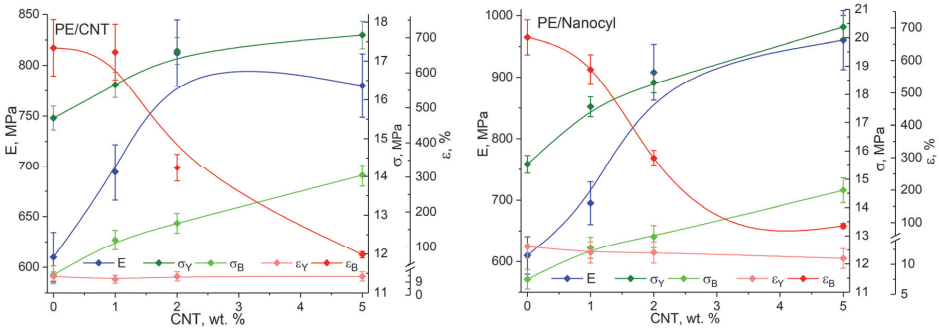

Fig. 9. PE/CNT and PE/Nanocyl nanocomposite tensile parameter *E*, σ_Y, σ_B, ε_Y and ε_B dependence on CNT concentration.

By comparing the simple mixing of CNTs in the PE matrix with the mixing of commercial PE/CNT concentrate (*Nanocyl*) in the PE matrix, it is possible to conclude that a greater effect on the *E* growth can be achieved by utilizing with *in situ* method obtained CNT masterbatch for PE nanocomposites, at 5 wt. % CNT concentration PE/*Nanocyl* showing 180 MPa higher *E* value than the PE/CNT nanocomposites. PE/*Nanocyl* nanocomposite ε_B values at 1 and 2 CNT wt. % were 87 % and 29 % lower than of the PE/CNT nanocomposites, but at 5 wt. % CNT content they slightly increased by 12 %. As other tensile parameters show, mechanical properties such as σ_Y, σ_B and ε_Y, despite the theoretically better CNT dispersion in *in situ* method obtained polymer/CNT concentrate, are quite similar to the melt mixed CNT composite σ_Y, σ_B, and ε_Y parameters, changing in 3 MPa, 0.6 MPa and 2 % borders.

PP/CNT and PET/CNT nanocomposites (Fig. 10) show a very rapid decrease in ε_B. The PP/CNT nanocomposites show the σ_Y peak after which PP/CNT samples with 2 and 5 wt. % CNT concentration immediately break. For PET/CNT nanocomposites, compared to the PET matrix, yielding was not observed as they broke already in the region of elastic deformation, showing a fragile fracture of up to 4 % in the deformation region.

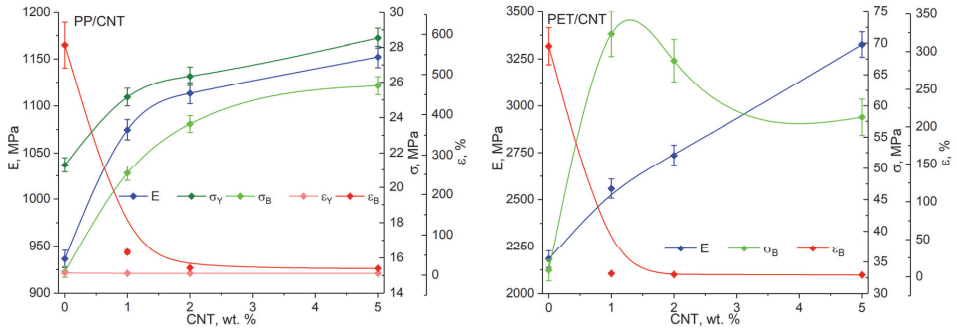

Fig. 10. PP/CNT and PET/CNT nanocomposite tensile parameter *E*, σ_Y, σ_B, ε_Y and ε_B dependence on CNT concentration.

It was determined that commercial PP and PET CNT masterbatches contribute to the nanocomposite E growth, however, very rapidly reduce ε_B values in comparison with, for example, the increase in the mechanical properties of nanocomposites obtained by the solution method. PP/CNT nanocomposite σ_B and σ_Y parameters increased in proportion to E increase, but ε_Y was virtually unaffected by CNT. For PET/CNT nanocomposites, σ_B decreased at CNT concentrations above 1 wt. % which was associated with a rapid decrease in ε_B.

Changes in the polymer/CNT nanocomposite E modulus, tensile strength σ_B and tensile yield strength σ_Y with respect to matrix parameters E_0, σ_{B0}, and σ_{Y0} depending on the CNT concentration are presented in Fig. 11.

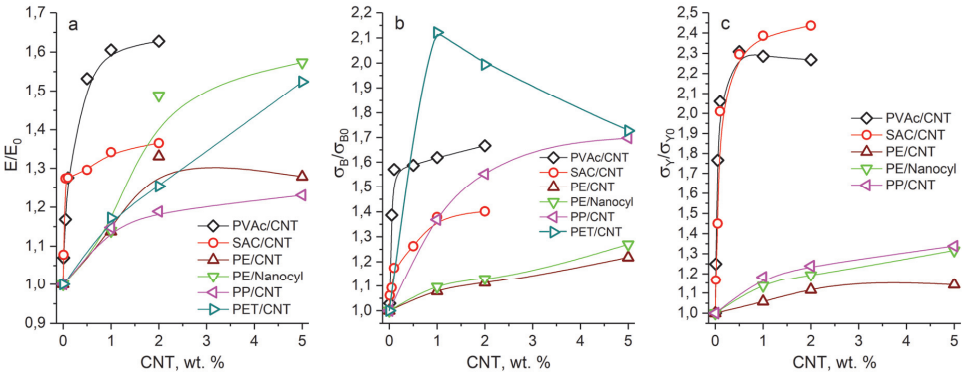

Fig. 11. Poliymer/CNT nanocomposite E modulus, tensile strength σ_B and tensile yield strength σ_Y relative values compared to polymer matrix.

Microhardness studies

PE/CNT, PE/Nanocyl, PP/ CNT and PET/CNT composite Vickers microhardness H_V dependence on filler concentration is shown in Fig. 12. PE/CNT, PE/Nanocyl, PP/CNT and PET/CNT composite σ_Y values were compared to H_V values (Table 4) according to Tabor's relation

$$H_V \approx k\sigma_Y . \qquad (8)$$

Given that the Vickers pyramid indenter is used, the constant k in equation (8) is usually in the range of 2–4. The yield strength σ_Y is taken as a reference value for the tensile stress [12]. Determined polymer/CNT nanocomposite H_V/σ_Y relations (Table 3) quite well match with theoretical k value, taking into account that in the literature various deviations from this correlation are mentioned [13]. The obtained data shows that microhardness measurements can be used for indicative assessment of σ_Y.

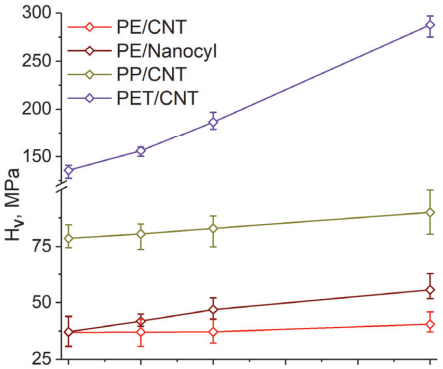

Fig. 12. Polymer/CNT nanocomposite H_V dependence on CNT concentration.

Table 4

Nanocomposite Vikers hardness H_V and σ_Y relation

CNT, wt. %	H_V/σ_Y			
	PE/CNT	PE/*Nanocyl*	PP/CNT	PET/CNT
0	3.1	3.1	3.4	2,1
1	2.4	2.3	3.2	*
2	2.1	2.6	3.3	*
5	2.8	2.8	3.4	*

* For these PET/CNT composites yield strength was not determined.

Impact strength studies

Investigated polymer/CNT nanocomposites under the influence of CNT filler showed reduction of their Charpy impact strength. Although in the polymer matrix dispersed CNTs could act as a reinforcement element, the nanocomposite impact strength was reduced or substantially did not change by increasing the CNT content as shown in Fig. 13, where the PE/CNT and PE/*Nanocyl* impact strength at –150 ºC, PP/CNT and PET/CNT impact resistance at room temperature is represented.

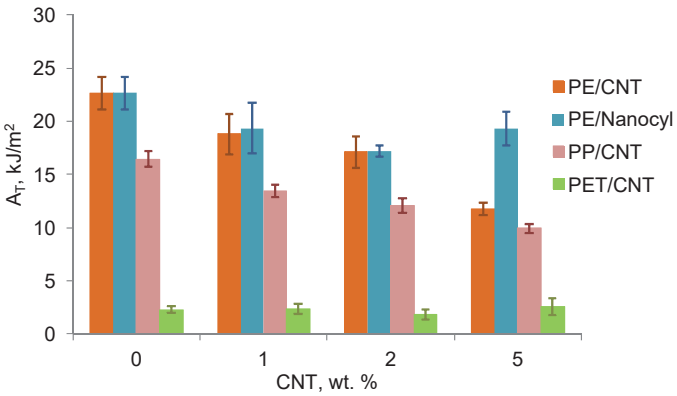

Fig. 13. Polymer/CNT nanocomposite impact strength depending on CNT content.

Due to the fact that the low impact energy was associated with the filler content, it can be seen that the highest filler content for all nanocomposites reduced the ability to absorb energy during crack propagation. This is the result of the fact that due to the high CNT surface energy and the high *l*/*d* ratio, it remains difficult to disperse CNTs in the polymer matrix at higher CNT contents. At the CNT agglomerate sites, a stress concentration points are formed in the polymer matrix, which act as a source of crack initiation. This leads to lower energy dissipation in the system, which, in addition to the existing microvoids between the CNTs and polymer matrix, during the impact causes microcracks followed by easy crack propagation.

The polymer nanocomposite impact force curves represented in Fig. 14 show that for all studied nanocomposite systems deflection is reducing by increasing the CNT concentration – samples are becoming increasingly fragile, although at the same time, the impact force slightly increases at lower deflection values. Therefore, despite the gradual reduction of the impact strength of nanocomposites, it is clear that part of the impact energy is directed to the CNT filler particles during the impact process.

Impact force curves of PE/CNT, PE/*Nanocyl* and PP/CNT samples show brittle failure (yielding followed by unstable cracking) but for PET/CNT nanocomposites splintering failure (unstable cracking followed by yielding) can be observed.

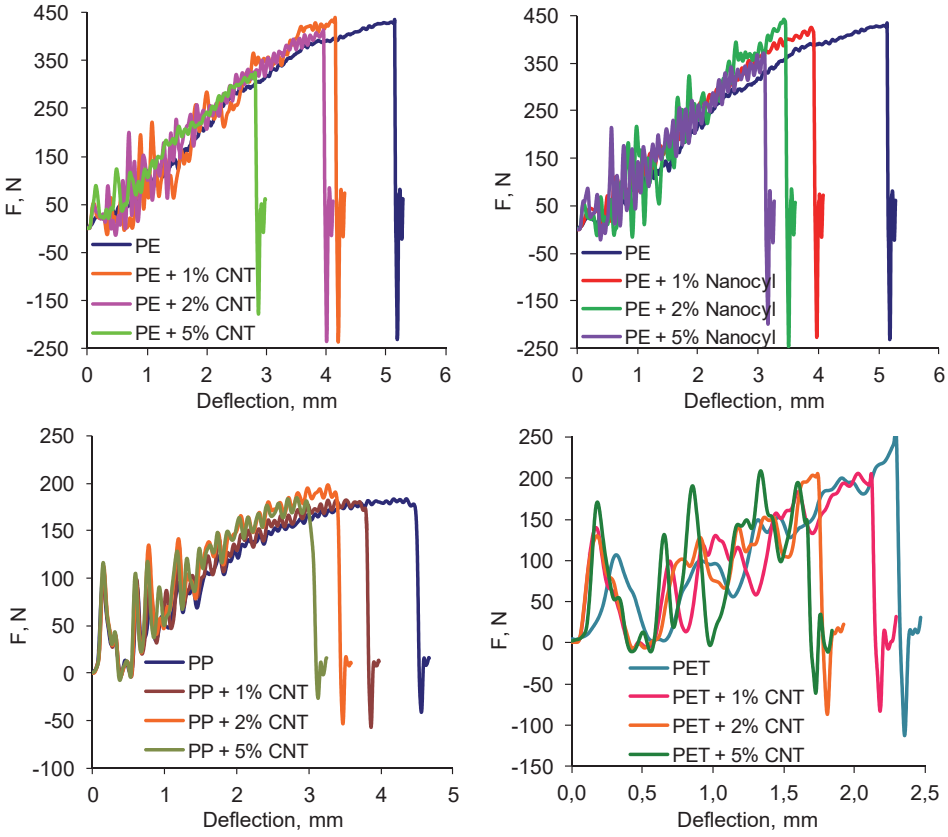

Fig. 14. Polymer/CNT nanocomposite impact force curves.

3. Thermal mechanical properties

By using the method of dynamic mechanical thermal analysis (DMTA), the determined storage modulus *E'* values of the investigated polymer/CNT nanocomposite gradually increased with an increase in CNT concentration, indicating the CNT reinforcing effect (Table 5).

Table 5

Storage modulus *E*' values determined with DMTA method at 23 ºC

CNT, wt. %	*E*', MPa					
	PVAc/CNT	SAC/CNT	PE/CNT	PE/*Nanocyl*	PP/CNT	PET/CNT
0	857	1075	888	888	1401	2390
0.5	1407	1141				
1	1772	1260	1001	1029	1740	2471
2	2259	1343	1033	1208	1840	2529
5			1133	1392	2049	2908

Table 6 shows the maximum values of the polymer/CNT nanocomposite loss modulus *E*" and the loss tangent tanδ, which characterizes the glass transition temperature T_g. It is evident that for the most polymer/CNT nanocomposites T_g tends to move in the direction of higher temperatures by increasing CNT content. Gradual increase in T_g shows that already small CNT filler into the polymer matrix begins to limit the mobility of polymer macromolecules.

Table 6

Glass transition temperatures T_g, ºC determined with DMTA method

CNT, wt. %	PVAc/CNT		SAC/CNT		PE/CNT		PE/*Nanocyl*		PP/CNT		PET/CNT	
	E"	tanδ	*E*"	tanδ	*E*"	tanδ	*E*"	tanδ	*E*"	tanδ	*E*"	tanδ
0	15	32	23	53	–109	–105	–109	–105	8	11	77	87
0.5	20	33	23	53								
1	23	35	23	53	–111	–112	–112	–108	8	10	79	86
2	26	40	26	55	–112	–110	–111	–107	10	10	78	86
5					–111	–108	–113	–108	8	11	81	87

4. Thermal properties

Differential scanning calorimetry of nanocomposites obtained by solution processing

Since PVAc and SAC are amorphous polymers, the changes in enthalpy associated with matrix glass transition were observed in differential scanning calorimetry (DSC) measurements of PVAc/CNT and SAC/CNT nanocomposites. PVAc/CNT and SAC/CNT nanocomposite glass transition temperatures T_g are shown in Fig. 15, which depicts that the CNT introduction leads to a shift in PVAc and SAC T_g to higher temperatures. PVAc/CNT nanocomposite T_g changed from 23 ºC of PVAc matrix up to 27 ºC at 2 wt. % CNT content and SAC/CNT nanocomposite T_g increased from 15 ºC of SAC matrix up to 19 ºC at 2 wt. % CNT content. It shows that there is a good CNT dispersion in PVAc

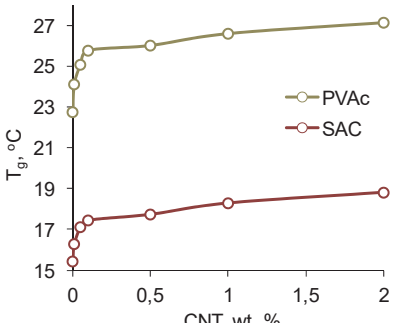

Fig. 15. Changes in PVAc/CNT and SAC/CNT nanocomposite T_g.

and SAC matrices and that strong interaction with polymer reduces the freedom of polymer macromolecule movement.

Differential scanning calorimetry of nanocomposites obtained by melt processing

Introduction of CNT fillers in PE, PP and PET matrices, as seen from the DSC cooling curves in Fig. 16, greatly accelerated the crystallization of melt processed nanocomposites, resulting in the crystallization peak shift to higher temperature range. CNTs also changed the characteristics of the melting peaks by shifting melting temperatures to higher ones (Fig. 16 b). The observed increase in the crystallization temperatures and the increase in melting temperatures without significant increase in the initial melting temperatures indicate that CNTs act as a crystallization agent, promoting faster growth of crystals and the formation of a large number of small crystallites in the heterogeneous crystallization process. It also points out that CNTs prevent the formation of large and uniform spherolites, which results in the formation of heterogeneous crystallites with a wide distribution of their size, impeding the formation of a densely ordered crystalline phase.

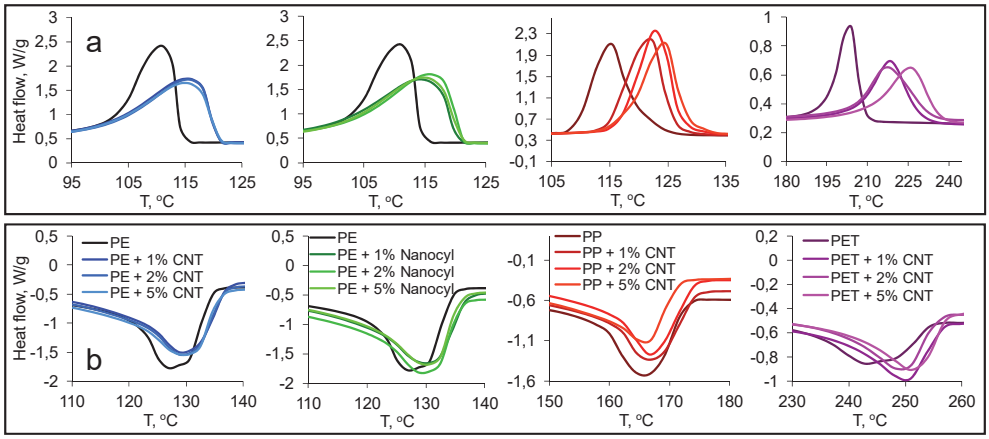

Fig. 16. Polymer/CNT nanocomposite DSC crystallization peaks in cooling cycle (a) and melting peaks in heating cycle (b).

Thermogravimetric analysis

The observed nanocomposite temperature at 50 % weight loss is summarized in Table 7. The thermal decomposition temperature at 50 % of weight loss is considered to be an indicator of the loss of the stability of the material structure. Although for the solution method obtained polymer/CNT nanocomposites CNTs had little effect on the thermal decomposition temperature, for the polymer/CNT nanocomposites obtained with melt processing, the weight loss temperatures moved to higher temperatures, indicating a higher thermal stability of nanocomposites, starting to decompose at higher temperatures. The improvement in thermal stability is associated with strong interphase effects between polymer and CNTs due to CNT network polymer matrix acting as a thermally insulating barrier, CNTs easily absorbing the supplied heat and evenly transfering it throughout the polymer matrix volume. As a result, the

CNT network barrier in the polymer matrix prevents thermal decomposition by improving heat transfer and preventing the release of thermal decomposition products.

Table 7

Polymer/CNT nanocomposite TGA temperature at 50 % weight loss

CNT, wt. %	PVAc/CNT	SAC/CNT	PE/CNT	PE/*Nanocyl*	PP/CNT	PET/CNT
0	352	414	469	469	454	440
0.01	357	416				
0.05	356	419				
0.1	356	419				
0.5	354	417				
1	353	419	488	495	463	440
2	352	423	490	499	465	443
5			496	500	464	446

Polymer/CNT nanocomposite thermal properties

Figure 17 a shows the thermal conductivity λ curves of polymer/CNT nanocomposites, which illustrates that compared to the polymer matrix by increasing the CNT concentration, the thermal conductivity of polymer/CNT nanocomposites increases. This occurs due to CNT high thermal conductivity (750 W/mK) [14]. The low λ values of polymer matrices are due to the flexible nature of the macromolecular chains and therefore the phonons produced by the heat fluctuations are spreading at lower speed than in crystalline materials.

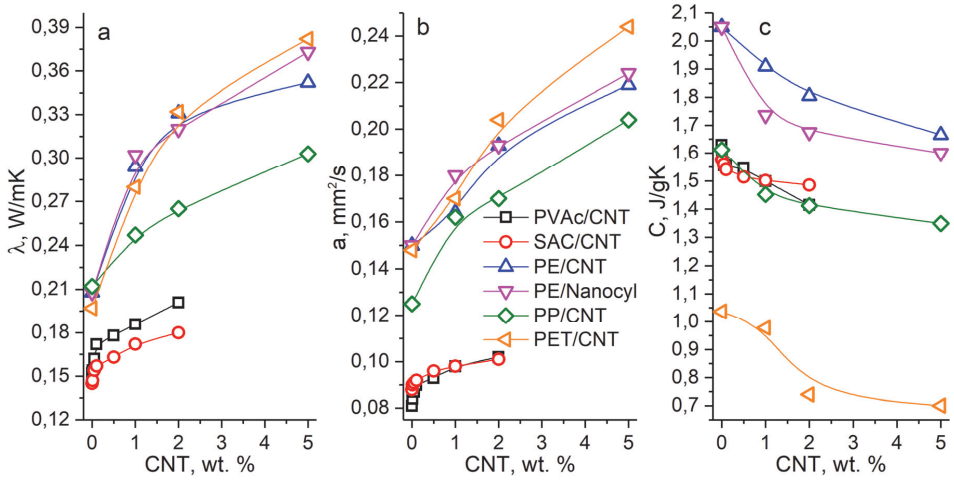

Fig. 17. Polymer/CNT nanocomposite thermal conductivity λ (a), thermal diffusivity *a* (b) and specific heat *c* (c) depending on CNT concentration.

Since phonons are also dominated in CNT heat transport, the thermal conductivity of polymer/CNT nanocomposites is strongly influenced by the phonon dispersion due to changes in their free path and scattering on the polymer matrix and the CNT boundary surface due to the large differences in thermal conductivity between these two components. The boundary resistance acts as a barrier to the heat flow between the polymer and CNT, thus the practical thermal conductivity of the studied composites is affected by high interphase resistance by the CNT-matrix or CNT-CNT boundary.

Crystalline polymers have longer phonon mean free path than glassy polymers due to their ordered structure, hence the amorphous PVAc and SAC nanocomposites showed the lowest thermal conductivity and thermal diffusuvity (Fig. 17 b). The thermal conductivity and thermal diffusivity and their increase with the addition of CNT for semi-crystalline PE, PP, and PET polymer nanocomposites were accordingly higher. If for PVAc/CNT and SAC/CNT nanocomposites at 2 wt. % CNT concentration, compared to matrix polymers, the thermal diffusivity increased by 26 % and 15 %, then at 2 wt. % CNT concentrations thermal diffusivity of PE/CNT, PE/Nanocyl, PP/CNT and PET/CNT nanocomposites increased by 29 %, 29 %, 36 % and 38 %.

The specific heat capacity *c* of the studied polymer/CNT nanocomposites (Fig. 17 c) differs from their thermal conductivity and thermal diffusivity. The addition of CNT reduces the specific heat capacity of polymer/CNT nanocomposites from relatively large matrix specific heat to the lower specific heat capacity values of CNT (0.75 J/gK) [14].

5. Dielectric properties

For investigated polymer/CNT nanocomposites (Fig. 18) two different AC conductivity σ' properties were observed depending on the CNT concentration. First of all, at low CNT concentrations, the AC conductivity σ' increased linearly with increasing frequency, thus showing a typical electrical insulating material behaviour. In contrast, at higher CNT concentrations, the polymer/CNT composite at low frequencies began to show an AC conductivity plateau with constant σ', which was no longer dependent on the frequency. Such independence of σ' from frequency and simultaneous increase by several orders of magnitude is already characteristic of electrically conductive materials, which suggests that at determined CNT concentrations the percolation threshold of the AC conductivity σ' is exceeded, which characterizes the conductive CNT network structure in the polymer matrix volume.

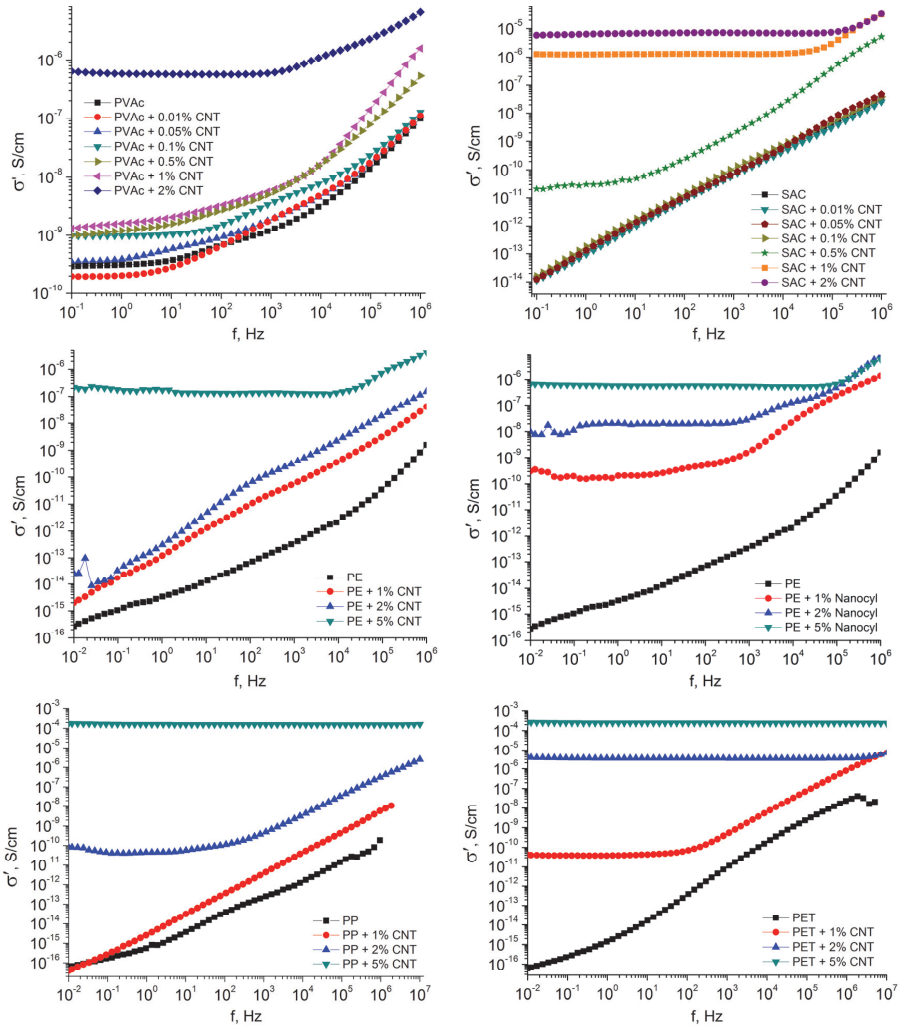

Fig. 18. Polymer/CNT nanocomposite AC conductivity σ' depending on frequency.

From SAC/CNT, PE/Nanocyl and PET/CNT nanocomposite (Fig. 19) theoretical calculations of the percolation threshold for DC, the statistical percolation theory can be used that determines the percolation concentration of filler at which the percolation threshold is observed. The CNT percolation concentration can be calculated by using the power law [15]:

$$\sigma_{DC} \approx \sigma_0 (\varphi - \varphi_\sigma)^{t_\sigma} \tag{9}$$

where σ_{DC} composite DC conductivity;

σ_0 CNT electrical conductivity;

φ CNT volume content;

φ_σ CNT percolation volume content;

t_σ exponent related to the system dimensionality.

The restrictions define that equation (9) can be used at low CNT concentrations (< 10 %) and above the percolation threshold ($\varphi > \varphi_\sigma$). The exponent t_σ values from 1–1.3 represent two-dimensional CNT conductive network and values from 1.6–2 – three-dimensional. Other CNT/polymer nanocomposite percolation threshold studies show φ_σ values from 0.0025 % to 10.5 % [16]. By increasing the CNT content above the φ_σ value, the CNT/polymer nanocomposite conductivity will gradually increase to reach the plateau.

In the case of AC conductivity, equation (9) can be applied to CNT concentrations below the critical frequency f_c, at which the sample AC conductivity σ' is no longer dependent on the frequency: $\sigma_{DC} = \sigma'(\omega \rightarrow 0)$. AC conductivity percolation concentration φ_σ was determined by representing the $\varphi - \varphi_\sigma$ volume concentration on the logarithmic scale, by gradually changing φ_σ until the highest R^2 value was reached. SAC/CNT, PE/Nanocyl and PET/CNT nanocomposite φ_σ values were obtained at 0.27 vol. % (0.49 wt. %), 0.4 vol. % (0.85 wt. %) and 0.67 vol. % (0.98 wt. %). At the calculated φ_σ values for SAC/CNT and PE/Nanocyl nanocomposites, the obtained exponent t_σ was 2.36 and for PET/CNT nanocomposites 2.44. The obtained t_σ values are greater than those defined in the theoretical CNT layout models in the polymer matrix. The frequently occurring higher t_σ values [17] are explained by the fact that such calculations are accurate at the filler concentration close to the percolation concentration. Moreover, since there is no direct physical contact between the CNTs, the conductivity is achieved due to the tunneling effect, in which case the large distribution of distances between the particles exhibits higher exponent t_σ and σ_0 values than theoretical 2D and 3D models.

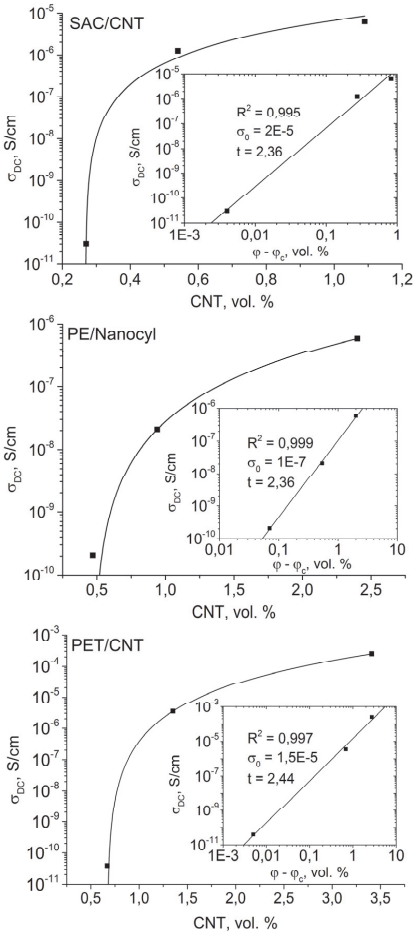

Fig. 19. SAC/CNT, PE/Nanocyl and PET/CNT nanocomposite electrical percolation parameters.

6. Rheological properties

The study of rheological properties gives insight into the internal structure and processability of polymers and their composites. These properties of CNT containing nanocomposites provide information on the structure of the CNT network, the dispersion of particles, and the effect between the CNT and the polymer matrix. By melt processing obtained PE/CNT, PE/Nanocyl, PP/CNT and PET/CNT nanocomposite complex viscosity η^*

dependence of the angular frequency ω in the oscillatory mode can be described using the Ostwald de Waele relationship [18] $\eta = K\dot{\gamma}^{n_{tec}-1}$, which according to Cox-Merz rule [19] $\eta(\dot{\gamma}) = |\eta^*(\omega)|_{\omega=\dot{\gamma}}$ can be applied for oscillatory mode to obtain viscosity values at high shear rates, which has a practical significance in polymer processing:

$$\eta^* = K\omega^{n_{tec}-1} \tag{10}$$

where K is consistency describing constant which is equal to effective viscosity value under normalized conditions (ω=1); n_{tec} is flow behaviour index, which characterizes the melt pseudoplasticity: Newtonian fluids $n_{tec} = 1$, pseudoplastic fluids $n_{tec} < 1$, dilatant fluids $n_{tec} > 1$.

Polymer/CNT system η*(ω) curves show two pseudoplastic regions indicating a change in the melt flow behaviour at higher ω values (Fig. 20). PE, PP and PET polymer melts had characteristics of the Newtonian fluid behaviour at low ω values with the calculated flow behaviour index $n_{tec} = 0.92 – 0.96$, but when the ω values increased above 30 rad/s, 1.3 rad/s and 20 rad/s, PE, PP and PET displayed pseudoplastic behaviour. Compared to polymer matrices, the effect of CNT on η * values for nanocomposites was much more pronounced in the pseudoplastic region at low angular frequencies than at high angular frequencies; by gradually decreasing n_{tec} values with increasing CNT concentration.

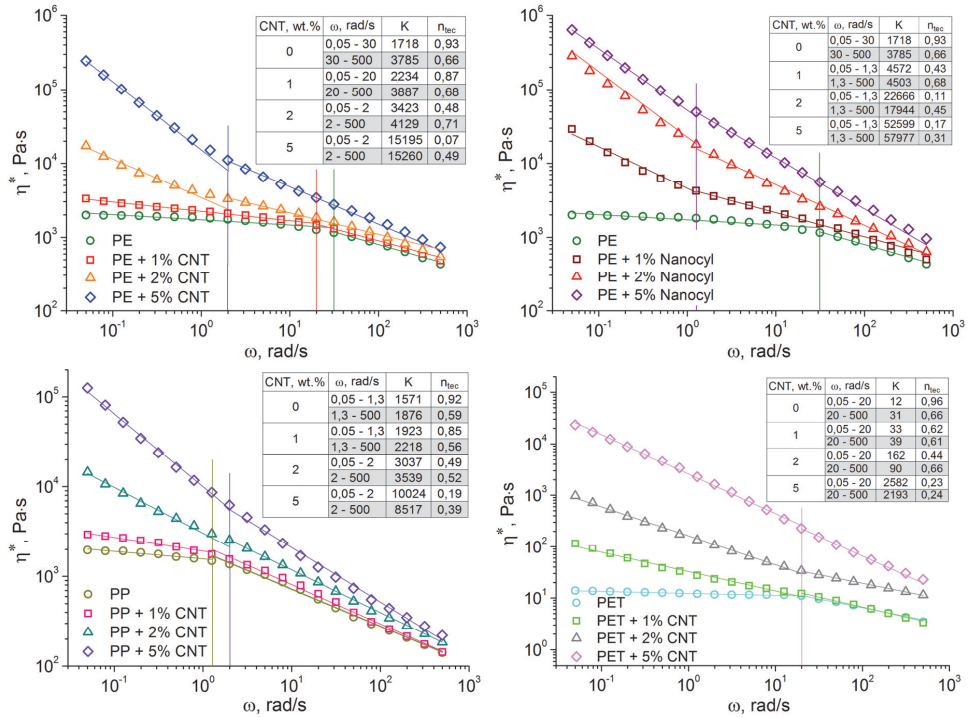

CNT, wt.%	ω, rad/s	K	n_{tec}
0	0,05 - 30	1718	0,93
	30 - 500	3785	0,66
1	0,05 - 20	2234	0,87
	20 - 500	3887	0,68
2	0,05 - 2	3423	0,48
	2 - 500	4129	0,71
5	0,05 - 2	15195	0,07
	2 - 500	15260	0,49

CNT, wt.%	ω, rad/s	K	n_{tec}
0	0,05 - 30	1718	0,93
	30 - 500	3785	0,66
1	0,05 - 1,3	4572	0,43
	1,3 - 500	4503	0,68
2	0,05 - 1,3	22666	0,11
	1,3 - 500	17944	0,45
5	0,05 - 1,3	52599	0,17
	1,3 - 500	57977	0,31

CNT, wt.%	ω, rad/s	K	n_{tec}
0	0,05 - 1,3	1571	0,92
	1,3 - 500	1876	0,59
1	0,05 - 1,3	1923	0,85
	1,3 - 500	2218	0,56
2	0,05 - 2	3037	0,49
	2 - 500	3539	0,52
5	0,05 - 2	10024	0,19
	2 - 500	8517	0,39

CNT, wt.%	ω, rad/s	K	n_{tec}
0	0,05 - 20	12	0,96
	20 - 500	31	0,66
1	0,05 - 20	33	0,62
	20 - 500	39	0,61
2	0,05 - 20	162	0,44
	20 - 500	90	0,66
5	0,05 - 20	2582	0,23
	20 - 500	2193	0,24

Fig. 20. Polymer/CNT nanocomposite complex viscosity η*(ω) curves.

Nanocomposite showing increase in η*, especially at 2 and 5 wt. % CNT concentrations in comparison with polymer matrices refers to the formation of connected or network structures as a result of CNT-CNT filler and CNT-polymer interaction. Such nanocomposite behaviour may also be related to the existence of friction between very anisotropic particles like CNTs due to their high *l*/*d* ratio. Therefore, nanocomposites showed a pronounced pseudoplastic fluid behaviour even at low ω values commonly observed for filled polymer compositions with a strong effect between the filler and polymer. The approximation of the investigated polymer/nanocomposite viscosity curves to the viscosity of polymer matrices at high ω values indicates that not only polymer intermolecular bonds collapse and macromolecules deform in the direction of flow, but also CNT and polymer macromolecule created structures collapse.

The dependence of the nanocomposite storage modulus (*G*') on ω (Fig. 21) shows that the PE, PP, and PET matrices indicated almost linear *G*' dependence on ω, while the polymer/CNT nanocomposite *G*' value dependence on ω decreased. A gradual decrease of nanocomposite *G*' curve slope by increasing the CNT content can be explained by the fact similar to the change in η * when the CNT-CNT or CNT-polymer interactions can lead to the formation of connected or network structures resulting in pseudoplastic fluid-like behaviour. Such a nanocomposite *G*' independence of ω at large CNT concentrations is considered to be a rheological percolation threshold.

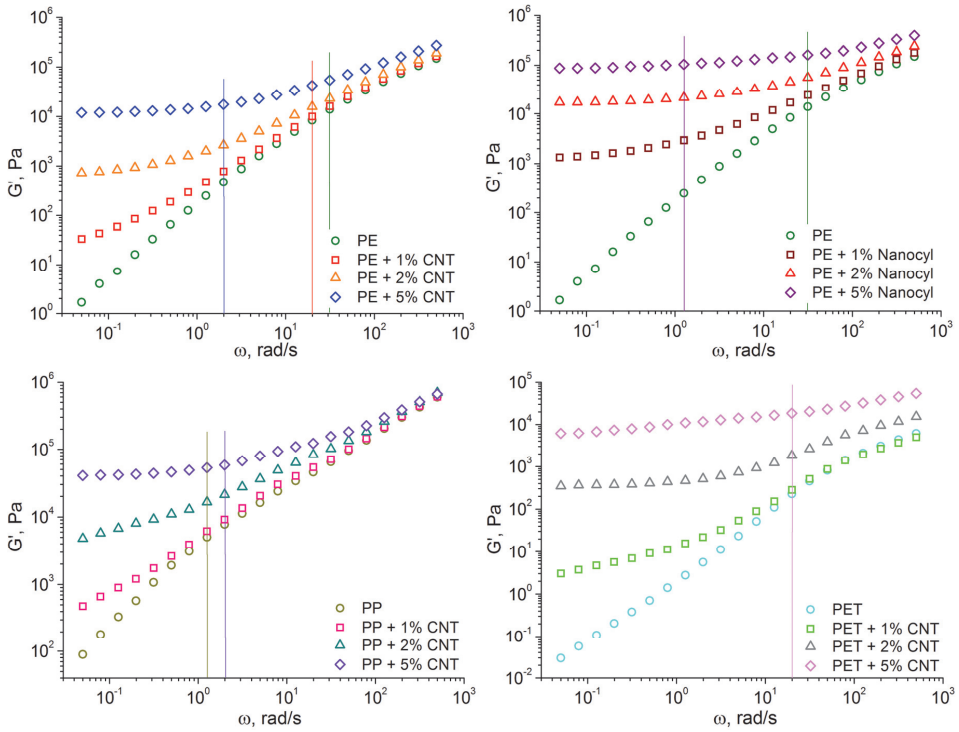

Fig. 21. Polymer/CNT nanocomposite storage modulus *G*'(ω) curves.

Similarly, as calculating the electrical percolation concentration, in order to calculate the rheological percolation concentration, it is possible to apply the percolation power law based on the variation of G' modulus, since the G' modulus most clearly describes the rheological changes of nanocomposites depending on the CNT concentration:

$$G' \approx G'_0\left(\varphi - \varphi_{c,G'}\right)^{t_{G'}} \tag{11}$$

where G' composite storage moulus;

G'_0 CNT characterizing storage modulus;

φ CNT volume content;

$\varphi_{c,G'}$ CNT percolation volume content;

$t_{G'}$ exponent related to the system dimensionality.

PE/CNT, PE/Nanocyl, PP/CNT and PET/CNT nanocomposite (Fig. 22) $\varphi_{c,G'}$ values were obtained at 0.4 vol. % (0.75 wt. %), 0.36 vol. % (0.67 wt. %), 0.39 vol. % (0.75 wt. %) and 0.64 vol. % (0.83 wt. %). Calculated PE/ Nanocyl and PET/CNT $\varphi_{c,G'}$ values are 0.15 and 0.18 wt. % lower than electrical percolation $\varphi_{c,\sigma}$ values. This is related to composite structure, wich is determined by interaction between macromolecules and CNTs. For electrical percolation, CNT network in a polymer matrix with CNT-CNT contacts is required, but in the case of rheological percolation, where the distances between CNTs are too large to form a connected CNT network in a matrix volume, G' increase is determined by the interaction of polymer-CNT in polymer melt, by CNT interfering with macromolecule movement. The obtained $t_{G'}$ values generally depend on the filler l/d ratio and angular frequency.

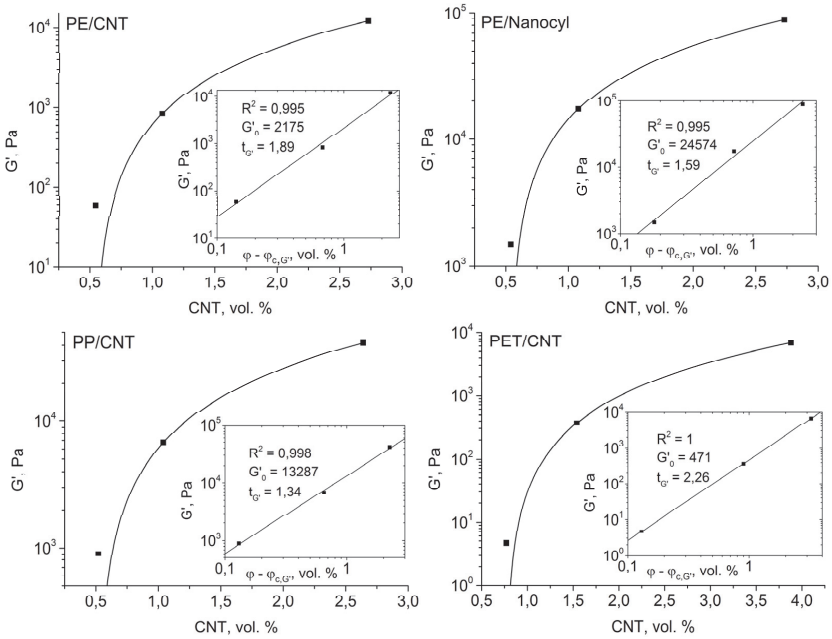

Fig. 21. Polymer nanocomposite rheological percolation parameters.

CONCLUSIONS

1. Polymer composites were obtained by making carbon nanotube (CNT) filler combination with thermoplastic polymers: polyvinylacetate (PVAc), styrene-acrylate copolymer (SAC), polyethylene (PE), polypropylene (PP) and polyethylene terephthalate (PET) in different technological forms: water dispersion and melt. The connection of parameters of stress-strain, electrical, rheological and thermal properties with characteristic parameters of the composite structure of the obtained composite was determined.
2. Technological solutions for combining have been found which guarantees satisfactory nanotube dispersion in a composite. When mixing in melt, some of the CNT aggregates are not completely destroyed. Separate CNT clusters in the polymer melt flow are stretched by mutual orientation of nanotubes. The resulting formations provide a significant reinforcing effect in the composite.
3. Nanotubes and their clusters efficiently reinforce all studied polymer matrices. The presence of small quantities (up to 2 wt. %) of nanotubes significantly changes the stress-strain properties of the matrices: the values of tensile and flexural elastic modulus increase, values of yield strength, ultimate strength and maximum flexural stress increase. Hardness of the composite increases and creep rate decreases.
4. By using the Mori-Tanaka mathematical model based on the idea of reinforcement-matrix flexible interaction the dependence of the nanocomposite elastic modulus on nanotube content in the composite, their mutual orientation and conformation is described.
5. Rapid change in stress-strain properties, sharp increase in thermal and electrical conductivity of the composites as well as the increase in the melt non-Newtonian nature with the increase of nanotube content in PE, PP and PET matrix composites, indicate the formation of network structures in a composite in which together with fiber-polymer interaction also fiber-fiber interaction is observed.
6. Due to the high thermal conductivity of nanotubes, their formed structures provide increased nanocomposite thermal conductivity and thermal diffusivity, but reduce their specific heat capacity.
7. Pronounced interphase polarization between the nanotube electroconductive network and the non conductive polymer matrix was observed. As a result, with increasing CNT content composite dielectric permittivity and dielectric loss rapidly increases. Composites acquire the properties of conductive materials.
8. When the content of nanotubes exceeds a certain limit, a percolation threshold is observed at which CNTs create a connected network structure. Percolation threshold is characterized by a rapid change in dielectric and rheological parameters.

REFERENCES

1. S. Iijima. Helical microtubules of graphitic carbon. *Nature*, 1991, 354, 56–58.
2. J. H. Lehman, M. Terrones, E. Mansfield, K. E. Hurst, V. Meunier. Evaluating the characteristics of multiwall carbon nanotubes. *Carbon*, 2011, 49 (8), 2581–2602.
3. A. G. Mamalis, L. O. G. Vogtländer, A. Markopoulos. Nanotechnology and nanostructured materials: trends in carbon nanotubes. *Precis. Eng.,* 2004, 28 (1), 16–30.
4. S. Yellampalli. Carbon nanotubes – Polymer Nanocomposites. Rijeka: InTech, 2011, 396 pp.
5. G. Pal, S. Kumar. Modeling of carbon nanotubes and carbon nanotube–polymer composites. *Prog. Aerosp. Sci.*, 2016, 80, 33–58.
6. J. L. Keddie. Film formation of latex. *Mat. Sci. Eng. R*, 1997, 21 (3), 101–170.
7. R. Hill. Elastic properties of reinforced solids; some theoretical principles. *J. Mech. Phys. Solids*, 1963, 11 (5), 357–372.
8. J. D. Eshelby. The determination of the elastic field of an ellipsoidal inclusion, and related problems. *Proc. R. Soc. A*, 1957, 241 (1226), 376–396.
9. T. Mori, K. Tanaka. Average stress in matrix and average elastic energy of materials with misfitting inclusions. *Acta Metall.*, 1973, 21 (5), 571–574.
10. A. Lagzdins, R. D. Maksimov, E. Plume. Anisotropy of elasticity of a composite with irregularly oriented anisometric filler particles. *Mech. Compos. Mater.*, 2009, 45 (4), 345–358.
11. D. M. Schaefer, R. S. Justice. How nano are nanocomposites? *Macromolecules*, 2007, 40 (24), 8501–8517.
12. I. M. Hutchings. The contributions of David Tabor to the science of indentation hardness. *J. Mater. Res.*, 2009, 24 (3), 581–589.
13. P. Zhang, S. X. Li, Z. F. Zhang. General relationship between strength and hardness. *Mater. Sci. Eng. A*, 2011, 529, 62–73.
14. S. Shenogin, L. Xue, R. Ozisik, P. Keblinski, D. G. Cahil. Role of thermal boundary resistance on the heat flow in carbon-nanotube composites. *J. Appl. Phys.*, 2004, 95 (12), 8136–8144.
15. W. Bauhofer, J. Z. Kovacs. A review and analysis of electrical percolation in carbon nanotube polymer composites. *Compos. Sci. Technol.*, 2009, 69 (10), 1486–1498.
16. W. Fang, H. W. Jang, S. N. Leung. Evaluation and modelling of electrically conductive polymer nanocomposites with carbon nanotube networks. *Composites Part B*, 2015, 83, 184–193.
17. M. Arjmand, M. Mahmoodi, G. A. Gelves, S. Park, U. Sundararaj. Electrical and electromagnetic interference shielding properties of flow-induced oriented carbon nanotubes in polycarbonate. *Carbon*, 2011, 49 (11), 3430–3440.
18. T. G. Mezger. The Rheology Handbook: For Users of Rotational and Oscillatory Rheometers. Hannover: Vincentz Network GmbH & Co KG, 2006, 299 pp.
19. W. P. Cox, E. H. Merz. Correlation of dynamic and steady flow viscosities. *J. Polym. Sci.*, 1958, 28 (118), 619–622.

APPROBATION OF THE DOCTORAL THESIS

Articles in Scientific Journals

1. **Bitenieks, J.**, Merijs-Meri, R., Zicāns, J., Kalniņš, M. Characterization of Polyvinyl Acetate/Multi Walled Carbon Nanotube Nanocomposites. *Key Eng. Mater.*, 2017, 721, 13–17. (Scopus)
2. Plyushch, A.O., Paddubskaya, A. G., Kuzhir, P.P, Maksimenko, S. A., Ivanova, T., Merijs-Meri, R., **Bitenieks, J.**, Zicans, J., Suslyaev, V. I., Pletnev, M. A. Comparative Analysis of Electromagnetic Response of PVA/MWCNT and Styrene-Acrylic Copolymer/MWCNT Composites, *Russ. Phys. J*+., 2016, 59 (2), 278–283. (Scopus)
3. Merijs-Meri, R., Zicans, J., Ivanova, T., **Bitenieks, J.**, Paddubskaya, A., Kuzhir, P., Maksimenko, S., Macutkevic, J., Kuznetsov, V., Moseenkov, S. Carbon Nanotubes and Carbon Onions for Modification of Styrene-Acrylate Copolymer Nanocomposites. *Polym. Compos.*, 2015, 36 (6), 1048–1054. (Scopus)
4. **Bitenieks, J.**, Merijs-Meri, R., Zicans, J., Maksimovs, R., Vasile, C., Musteata, V. E., Styrene-acrylate/carbon nanotube nanocomposites: Mechanical, thermal, and electrical properties, *Proc. Est. Acad. Sci.*, 2012, 61 (3), 172–177. (Scopus)
5. Maksimov, R. D., **Bitenieks, J.**, Plume, E., Zicans, J., Merijs-Meri, R., Properties of a Composite Prepared Using a Concentrate of Carbon Nanotubes in Polyethylene. *Mech. Compos. Mater.*, 2012, 48 (1), 47–56. (Scopus)
6. Merijs-Meri, R., **Bitenieks, J.**, Kalnins, M., Maksimov, R., Modeling and Stress-Strain Characteristics of Mechanical Properties of Carbon Nanotube Reinforced Polyvinylacetate Nanocomposites. *J. Appl. Polym. Sci.*, 2011, 122 (6), 3569–3573. (Scopus)
7. Maksimov, R. D., **Bitenieks, J.**, Plume E., Zicans, J., Merijs-Meri, R., The Effect of Introduction of Carbon Nanotubes on the Physicomechanical Properties of Polyvinylacetate. *Mech. Compos. Mater.*, 2011, 46 (3), 237–250. (Scopus)

Full-Text Conference Papers

1. **Bitenieks, J.**, Merijs-Meri, R., Zicāns, J., Kalniņš, M. Mechanical Properties of Polyethylene/Multi-Walled Carbon Nanotube Nanocomposite. In: Riga Technical University 57th International Scientific Conference "Materials Science and Applied Chemistry" (MSAC 2016): Proceedings and Programme, Latvia, Riga, 21–21 October, 2016. Riga: RTU Press, 2016, 36–39.
2. Merijs-Meri, R., Zicāns, J., Ivanova, T., **Bitenieks, J.**, Kuzhir, P., Maksimenko, S., Kuznetsov, V., Moseenkov, S. Carbon Nanotubes and Carbon Onions for Modification of Styrene-Acrylate Copolymer Based Nanocomposites. In: AIP Conference Proceedings: 7th International Conference on Times of Polymers (TOP) and Composites, Italy, Ischia, 22–26 June, 2014. Melville: American Institute of Physics, 2014, 426–429. (Scopus)
3. Zicans, J., Merijs-Meri, R., Ivanova, T., **Bitenieks, J.**, Maksimovs, R, Vasile, C, Musteata, V. E., Structure, elastic and electrical properties of polyethylene (PE)/carbon nanotube (CNT) nanocomposites, ECCM 2012 – Composites at Venice, Proceedings of the 15th European Conference on Composite Materials 2012, 15th European Conference on

Composite Materials: Composites at Venice, ECCM 2012. Venice, Italy, 24–28 June, 2012, 1–8. (Scopus)

4. **Bitenieks, J.**, Ivanova, T., Merijs-Meri, R., Kalniņš, M., Maksimovs, R. Carbon Nanotube/Polyvinyl Acetate Composites: Structure and Stress-Strain Characteristics. In: Proceedings of 14th European Conference on Composite Materials, Hungary, Budapest, 7–10 June, 2010. Budapest: 2010, 1–6.
5. Merijs-Meri, R., **Bitenieks, J.**, Kalniņš, M., Maksimovs, R. Modeling and Stress-Strain Characteristics of Mechanical Properties of Carbon Nanotube Reinforced Polyvinylacetate Nanocomposites. In: AIP Conference Proceedings: 5th International Conference on Times of Polymers (TOP) and Composites, Italy, Ischia, 20–23 June, 2010. Melville: American Institute of Physics, 2010, Vol. 1255, 333–335. (Scopus)
6. Ivanova, T., **Bitenieks, J.**, Merijs-Meri, R., Zicāns, J., Roja, Ž., Bledzki, A. Characterization of CNT- Polymer Nanocomposites Prepared by Latex Technology. In: Scientific Proceedings of the International Conference "MITECH 2009", Czech Republic, Prague, 25–26 June, 2009. Prague: Czech University of Life Sciences Prague, 2009, 96–101.
7. Elksnite, I., **Bitenieks, J.**, Zicans, J., Bledzki, A. K., Manufacturing and investigation of the MWCNT/Polymer Nanocomposites, EMRS Symposium F: Nanocomposite Materials; Warsaw; Poland; 15–19 September, 2008. *Solid State Phenomena*, 2009, 151, 171–175. (Scopus)

Participation in International Conferences

1. **Bitenieks, J.**, Merijs-Meri, R., Zicāns, J., Kalniņš, M. Characterization of Polyvinyl Acetate/Multi Walled Carbon Nanotube Nanocomposites. In: The 25th International Baltic Conference of Engeneering Materials & Tribology Baltmattrib 2016: Book of Abstracts, Latvia, Riga, 3–4 November, 2016. Riga: The Latvian Materials Research Society, 2016, 78–78.
2. **Bitenieks, J.**, Merijs-Meri, R., Zicāns, J., Kalniņš, M. Mechanical and Electrical Characteristics of Polyethylene/Carbon Nanotube Nanocomposite. In: Baltic Polymer Symposium 2016: Programme and Abstracts, Lithuania, Klaipeda, 21–24 September, 2016. Kaunas: 2016, 32–32.
3. Ivanova, T., Zicāns, J., **Bitenieks, J.**, Merijs-Meri, R., Maksimenko, S., Kuzhir, P. The Effect of Anisomeric Carbonaceous Nanofillers on the Relaxational Behaviour of Thermoplastic Polymers. In: Baltic Polymer Symposium 2013: Pogramme and Abstracts, Lithuania, Trakai, 18–21 September, 2013. Vlnius: Vilnius University Publishing House, 2013, 53–53.
4. **Bitenieks, J.**, Trausa, A., Merijs-Meri, R., Zicāns, J., Ivanova, T., Kužir, P., Maksimenko, S. The Effect of Anisometric Carbon Nanofillers on the Structural, Electrical and Mechanical Properties of Thermoplastic Polymer Nanocomposites. In: Abstracts of Riga Technical University 54th International Scientific Conference: Section: Materials Science and Applied Chemistry, Latvia, Riga, 14–16 October, 2013. Riga: RTU Press, 2013, 70–70.

5. Merijs-Meri, R., Zicāns, J., Ivanova, T., **Bitenieks, J.**, Maksimenko, S., Kuzhir, P. Characterization of Carbon Nanofillers Containing Composites Obtained by Means of Latex Based Route. In: BALTTRIB 2013: VII International Scientific Conference: Extended Abstracts, Lithuania, Kaunas, 14–15 November, 2013. Kaunas: Aleksandras Stulginkis University, 2013, 40–41.
6. Merijs-Meri, R., Zicāns, J., Ivanova, T., **Bitenieks, J.**, Kaļķis, V. Structure, Elastic and Thermophysical Properties of Styrene-Acrylate Polymer/Nanostructured Carbon Composites. In: 17th International Conference on Composite Structures: Book of Abstracts, Portugal, Porto, 17–21 June, 2013. Porto: 2013, 104–104.
7. Zicāns, J., Merijs-Meri, R., Ivanova, T., **Bitenieks, J.**, Maksimovs, R., Vasile, C., Musteata, V. Structure, Elastic and Electrical Properties of Polyethylene (PE)/Carbon Nanotube (CNT) Nanocomposites. In: Electronic Proceedings of the International Conference – 15th European Conference on Composite Materials. Comoposites at Venice, Italy, Venice, 24–28 June, 2012. Venice: 2012, 1–1.
8. **Bitenieks, J.**, Merijs-Meri, R., Zicāns, J., Maksimovs, R., Plūme, E. Physicomechanical Properties of Polyethylene/Carbon Nanotube Composite Prepared Using Concentrate of Nanotubes in Polyethylene. In: Seventeenth International Conference "Mechanics of Composite Materials" (MCM – 2012): Book of Abstracts, Latvia, Riga, 28 May – 1 June, 2012. Riga: 2012, 61–61.
9. Zicāns, J., Merijs-Meri, R., **Bitenieks, J.**, Maksimovs, R., Knite, M. Mechanical and Electrical Properties of PE Nanocomposites with Carbon Nanotubes. In: International Conference "Functional Materials and Nanotechnologies" (FM&NT-2012): Book of Abstracts, Latvia, Riga, 17–20 April, 2012. Riga: 2012, 257–257.
10. Zicāns, J., Merijs-Meri, R., **Bitenieks, J.**, Ivanova, T., Kaļķis, V., Vasile, C., Musteata, V. Structure, Elastic and Relaxation Behavior of Styrene-Acrylate Polymer/Multiwall Carbon Nanotubes Composites. In: XI International Conference of Nanostructured Materials (NANO2012): CD of Abstracts, Greece, Rhodes, 26–31 August, 2012. Rhodes: 2012, 1–1.
11. **Bitenieks, J.**, Merijs-Meri, R., Zicāns, J., Maksimovs, R., Vasile, C., Musteata, V., Cheaburu, C. Styrene-Acrylate/CNT Nanocomposites: Structure and Selected Exploitation Properties. In: Book of Abstracts of the International Conference Baltic Polymer Symposium 2011, Estonia, Parnu, 21–24 September, 2011. Parnu: 2011, 33–33.
12. Zicāns, J., **Bitenieks, J.**, Knite, M. Carbon Nanotubes Modified Polyvinylacetate Composite: Theoretical and Experimental Aspects. In: Book of Abstracts of 16th International Conference on Composite Structures (ICCS16), Portugal, Porto, 28–30 June, 2011. Porto: 2011, 409–409.
13. **Bitenieks, J.**, Zicāns, J., Merijs-Meri, R., Ivanova, T., Knite, M., Maksimovs, R. Structure and Properties of Polymer-Carbon Nanotube Composites, Obtained by Latex Route. In: Abstracts of the 52nd International Scientific Conference of Riga Technical University. Section: Materials Science and Applied Chemistry, Latvia, Riga, 13–14 October, 2011. Riga: RTU, 2011, 60–60.

14. Zicāns, J., Merijs-Meri, R., Ivanova, T., **Bitenieks, J.**, Vasile, C., Musteata, V. Structure and Functional Properties of Polymer-Carbon Nanotube Composites. In: Book of Abstracts of International Workshop "Characterization of Safe Nanostructured Polymeric Materials", Italy, Pozzuoli, Naples, 3–4 March, 2011. Pozzuoli: 2011, 71–71.
15. Zicāns, J., Merijs-Meri, R., Ivanova, T., **Bitenieks, J.**, Knite, M. Structure and Electrical Properties of Styrene Acrylonitrile Copolymer Nanocomposites. In: International Conference "Functional Materials and Nanotechnologies" (FM&NT-2011): Book of Abstracts, Latvia, Riga, 5–8 April, 2011. Riga: University of Latvia, 2011, 76–76.
16. **Bitenieks, J.**, Zicāns, J., Merijs-Meri, R. Rheological, Elastic and Dielectric Properties of Polyethylene/Carbon Nanotube Nanocomposites. In: International Workshop "Characterization of Safe Nanostructured Polymeric Materials": Book of Abstracts, Italy, Pozzuoli (Naples), 3–4 March, 2011. Pozzuoli: 2011, 38–38.
17. **Bitenieks, J.**, Merijs-Meri, R., Zicāns, J., Maksimovs, R. Carbon Nanotube Containing Polymer Nanocomposites: Structural, Rheological and Mechanical Behaviour. In: Baltic Polymer Symposium 2010: Programme and Abstracts, Lithuania, Palanga, 8–11 September, 2010. Kaunas: Technologija, 2010, 7–7.
18. **Bitenieks, J.**, Ivanova, T., Merijs-Meri, R., Kalniņš, M., Maksimovs, R. Carbon Nanotube/Polyvinyl Acetate Composites: Structure and Stress-Strain Characteristics. In: 14th European Conference on Composite Materials, Hungary, Budapest, 7–10 June, 2010. Budapest: Budapest University of Technology and Economics, 2010, 6–6.
19. **Bitenieks, J.**, Zicāns, J., Maksimovs, R., Merijs-Meri, R., Plūme, E. Physicomechanical Properties of Polyvinylacetate Reinforced with Carbon Nanotubes. In: Sixteenth International Conference "Mechanics of Composite Materials" (MCM – 2010): Book of Abstracts, Latvia, Riga, 24–28 May, 2010. Riga: Institute of Polymer Mechanics. University of Latvia, 2010, 51–51.
20. Maksimovs, R., Zicāns, J., Bledzki, A., Ivanova, T., **Bitenieks, J.** Polyvinylacetate/CNT Nanocomposites for Coating Applications. In: Extended Abstracts of the International Conference Balttrib 2009, Lithuania, Kaunas, 19–21 November, 2009. Kaunas: LU of Agriculture, 2009, 23–23.
21. **Bitenieks, J.**, Merijs-Meri, R., Maksimovs, R., Plūme, E. Properties of Carbon Nanotube-Reinforced Polymer Composite. In: Baltic Polymer Symposium 2009: Programme and Proceedings, Latvia, Ventspils, 22–25 September, 2009. Riga: RTU, 2009, 34–34.

Juris Bitenieks was born in Valmiera in 1985. He received the Bachelor degree of Engineering Science in Materials Science in 2007 and the Master degree of Engineering Science in Materials Science in 2009 from Riga Technical Universty (RTU).

Since 2006, he has worked in RTU Institute of Polymer Materials where he is carrying out the research on properties of polymer composite materials and development of their processing technologies.